VOLUME 18, 1956/57, No. 10 pp. 285-316 Published 23rd March 1957

Philips Technical Review

DEALING WITH TECHNICAL PROBLEMS
RELATING TO THE PRODUCTS, PROCESSES AND INVESTIGATIONS OF
THE PHILIPS INDUSTRIES

EDITED BY THE RESEARCH LABORATORY OF N.V. PHILIPS' GLOEILAMPENFABRIEKEN, EINDHOVEN, NETHERLANDS

FERROXCUBE MATERIAL FOR PIEZOMAGNETIC VIBRATORS

by C. M. van der BURGT.

621.318.134:621.372.412

For generating and detecting ultrasonic waves use is frequently made of piezoelectric or piezomagnetic (magnetostrictive) vibrators. For piezomagnetic vibrator cores, specially prepared types of ceramic ferroxcube have proved in many respects to be as good as, and in some respects even superior to the piezomagnetic metals and alloys that have hitherto commonly been used. Ferroxcube vibrators can be used not only for generating and detecting acoustic waves, but also as temperature-independent elements in electric band-pass filters. Special types of ferroxcube have likewise been developed for this purpose.

Introduction

In this article we shall be principally concerned with the generation and detection of ultrasonic waves in a surrounding liquid or solid medium. It will hardly be necessary to dwell at length on the great importance that this technique has acquired in recent years. It is used, for example, in under-water signalling (echo-sounding, "Asdic", "Sonar"); for flaw detection in solid materials; for cleaning small mechanical components; for the working of materials, e.g. drilling glass and other brittle materials [1]; for soldering aluminium (the film of oxide is shattered as it forms); and for therapeutic purposes. [2]

The ultrasonic vibrators employed in all the above instances belong to the category of transducers which convert electrical energy into mechanical or acoustical energy and vice versa. In this respect they can be compared with loudspeakers and microphones which serve to generate and detect sound waves in air in a frequency range between 20 c/s and 20 kc/s.

In the moving-coil loudspeaker, the conversion of electrical into acoustical energy is based upon the forces, which act on a coil through which the signal current is passed, the coil being located in the field of a permanent magnet. These forces set a membrane (loudspeaker cone) in motion, whereby sound waves are created in the surrounding medium. In principle a loudspeaker can also be made to work as a microphone: when the cone is set vibrating by sound waves, voltages are induced in the coil, i.e. acoustical energy is converted into electrical energy.

Electrodynamic systems cannot in general be used to generate and detect ultrasonic waves (frequencies above 20 kc/s) in liquids or solids; for this purpose vibrators of piezoelectric or piezomagnetic materials are indicated. This article concerns piezomagnetic vibrators, but because of the close analogy with piezoelectric vibrators, it will be useful to begin with a brief discussion of the latter [3]).

A piezoelectric vibrator may consist, for example, of a quartz crystal which is exposed to an alternating electric field and consequently undergoes periodic alterations in shape. Such a piezo-vibrator is mostly used at a frequency close to one of the mechanical resonance frequencies of the vibrating body. In the piezoelectric effect of quartz and a number of other crystals, such as ammonium dihydrogen phosphate (ADP), lithium sulphate hydrate (LSH) and potassium sodium tartrate (Rochelle salt), which are used as single crystals, the deformation is an odd function of the electrical field strength and changes in sign with the latter. The deformation of the first three crystals named is proportional to the field strength even up to high values of the latter. (In the case of Rochelle salt which shows marked hysteresis, there is no such simple proportionality.) There are polycrystalline materials, moreover, such as the ceramic materials: barium titanate ($BaTiO_3$) and lead titanate-zirconate ($PbTi_{1-z}Zr_zO_3$) which are also deformed by an electric field; here, however, deformation is an even function of the field strength, i.e. for a given field strength it is independent of the sign of the field. Such materials, for which of course there is no proportionality between field and deformation, can be rendered "linear" for small alternating fields by imparting them with a biasing polarization. This is done by subjecting them to a constant field on which the low-amplitude alternating field is superimposed. In some cases the polarizing field can be dispensed with, viz. when "remanent electric polarization" can be used.

---

[1] An article on ultrasonic drilling will appear in the next issue of this Review.

[2] See, for example, Technical aspects of sound, Vol. II, editor E. G. Richardson, Elsevier, Amsterdam 1957; T. F. Hueter and R. H. Bolt, Sonics, Wiley & Sons, New York 1955; L. Bergmann, Der Ultraschall, Hirzel Verlag, Zürich, 6th ed. 1954.

[3] Regarding piezoelectricity, see e.g. J. C. B. Missel, Piezoelectric materials, Philips tech. Rev. 11, 145-150, 1949/50.

Let us now compare the above with the piezomagnetic vibrators which can be used for generating and detecting ultrasonic waves [4]). These vibrators are based on a piezomagnetic effect (magnetostriction) of pre-magnetized (polarized) ferromagnetic materials. This piezomagnetic effect is a linear effect, comparable with the linear piezoelectric effect of polarized barium titanate. In principle all pre-magnetized ferromagnetic materials show this piezomagnetic effect.

To meet the various applications mentioned above, special ferromagnetic materials have been developed whose piezomagnetic effects are particularly pronounced. Initial development work consisted in a search for metals and metal alloys which would fit the purpose, such as nickel, "Permalloy" (Ni, Fe), "Alfer" and "Alfenol" (Al, Fe), and "Vanadium-Permendur" (V, Co, Fe). To generate vibrations, these materials have to be placed in a rapidly alternating magnetic field, and consequently they must be laminated. If they are not, the eddy currents produced (skin effect) lead to serious weakening of the magnetic field inside the material and thus diminish the resultant piezomagnetic effect.

In recent years ceramic materials have been developed on a wide scale (e.g. the nickel-zinc ferrites, ferroxcube 4), which can be employed as cores in coils, transformers, etc. for use at very high frequencies [5]). Because of their high electric resistivity these materials need not be laminated. Thus the idea arose of investigating whether such materials could not with advantage be used for ultrasonic piezomagnetic applications.

This was found to be so. The varieties of ferroxcube developed by Philips have been found to be particularly good materials for piezomagnetic vibrators, especially if certain changes are introduced in their chemical composition and method of preparation. The brittleness inherent in ceramics does, it is true, set a limit to the maximum power that can be radiated; but for ferroxcube this limit is high enough for most practical purposes. These new ferroxcube materials can be used both for radiators and for detectors.

Let us return for a moment to the piezoelectric vibrators. Some piezoelectric crystals, such as quartz, possess a high mechanical Q and hence exhibit strong resonance at a certain sharply defined frequency when an alternating electrical field is applied. This has led to another, non-acoustic application, viz. to their use as the selective components of electrical filters and frequency stabilizers in oscillating circuits. An important feature of such circuits is that the vibration frequency must be independent of temperature. With quartz resonators this is very nearly the case. The constancy can be still further improved by cutting the plate from the crystal in a special manner [6]) (with a prescribed orientation relative to the crystallographic axes).

The question arose as to whether piezomagnetic materials and more particularly ferroxcube could, like piezo-quartz, be applied as elements in electric filters requiring both a high mechanical Q and a reasonably strong piezomagnetic effect. With ferroxcube, but not with the piezomagnetic metals, this has indeed been found possible. Here again an important factor is the temperature independence of the resonance frequency. Further investigation has shown that the behaviour of ferroxcube resonators towards variations in temperature is influenced by the presence of cobalt. It has been found possible with ferroxcubes that do not possess the desired temperature independence to give them the required constancy by adding small amounts of cobalt.

---

[4]) Piezomagnetism is a new term coined to cover the various reversible magnetomechanical phenomena commonly included under magnetostriction (see for example G. Bradfield, Ultrasonic electro-acoustics: General review, Acustica 4, 171-181, 1954). A comprehensive historical survey of the application of piezomagnetic vibrators can be found in F. V. Hunt's Electroacoustics, Harvard Univ. Press, Cambridge (Mass.) 1954.

[5]) J. J. Went and E. W. Gorter, The magnetic and electrical properties of ferroxcube materials, Philips tech. Rev. **13**, 181-193, 1951/52.

[6]) W. Parrish, The manufacture of quartz oscillator-plates, Philips tech. Rev. **11**, 323-332, 351-360, 1949/50, and **12**, 166-176, 1950/51.

In what follows we shall first briefly discuss piezomagnetism and the working conditions of piezomagnetic vibrators; we shall then go on to examine in greater detail the properties of the new ferroxcube materials for the various applications enumerated above and how those properties are influenced by the manner of preparation and the composition.

The treatment will be kept as simple as possible. For a more exhaustive analysis the reader is referred to recent publications [7]), where fuller references to the literature can also be found, and to an article later to appear in this journal which will be devoted to the theoretical aspects of the matter here discussed.

Some remarks on piezomagnetism

The magnetism of a ferromagnetic material is caused by the spin vectors of certain groups of electrons. Viewed "microscopically" the material consists of small regions (Weiss domains) in which the spins are more or less parallel below a certain temperature (Curie temperature) and cause a temperature-dependent spontaneous magnetic polarization. If we consider a single crystal which is so small that it contains only one Weiss domain, then a change in the orientation of the spins brought about by an external magnetic field will result in a change in the forces between the atoms. The shape of the crystal will then be changed. If this deformation is opposed by neighbouring crystals, for example when the crystal forms part of a polycrystalline material, internal stresses will be set up in the crystal. If, conversely, the crystal is subjected to external stresses, it will not only be elastically deformed, but moreover, there will be a change in the orientation of the spin vectors and hence a change in the state of magnetization. The relationship between the orientation of the spins, the elastic deformation and the internal and external stresses in a crystal forming part of a polycrystalline material is a complex one. We shall therefore forgo any attempt at a detailed description of the microscopic state of a piezomagnetic material and shall confine ourselves to the macroscopically perceptible changes.

Let us suppose that we are dealing with a homogeneous polycrystalline, isotropic material. Then the deformation of a rod which is magnetized from the virgin state along its axis, can be described in the usual way by a roughly quadratic relation between the induction [8]) B and the change in length Δl thereby produced. This relationship which was touched upon in the introduction is shown graphically in *fig. 1* for a number of materials; the tensile strain $\varepsilon = \Delta l/l$ is plotted against B. A property of all the curves is that they approximately follow the B axis in the vicinity of the origin. For a number of iron alloys and for ferrous ferrite (magnetite, $Fe^{2+}Fe_2^{3+}O_4$), ε is positive (positive magnetostriction). ε is also found to be positive for pure iron, at least for not too high values of B; near the saturation point of iron, ε changes sign.

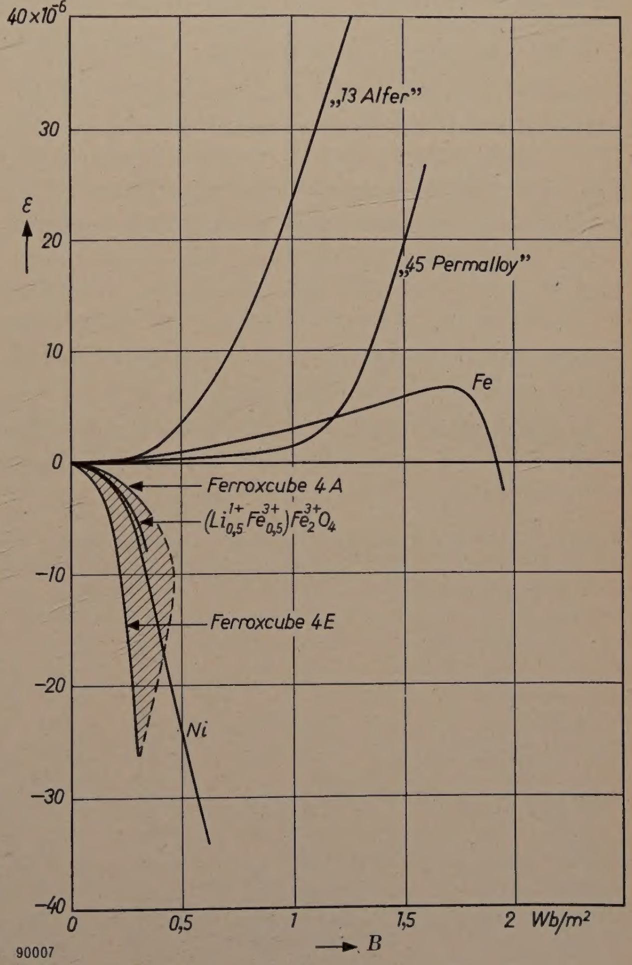

Fig. 1. Fractional change in length $\varepsilon = \Delta l/l$ for piezomagnetic materials, as a function of B ($\approx J$). Virgin curves.

---

[7]) C. M. van der Burgt, Dynamical physical parameters of the magnetostrictive excitation of extensional and torsional vibrations in ferrites, Philips Res. Rep. **8**, 91-132, 1953. C. M. van der Burgt, Performance of ceramic ferrite resonators as transducers and filter elements, J. Acoust. Soc. Amer. **28**, 1020-1032, 1956.

[8]) It would be more exact to call it the magnetic polarization $J (= B - \mu_0 H)$. The difference between J and B, however, can in practice be ignored owing to the fairly high (relative) permeability. Moreover, from a technical point of view, B is the more interesting quantity.

Negative values of ε are found for pure nickel and for various types of ferroxcube. In the figure the ε-B curves for ferroxcube 4A($(Ni_{0.35}Zn_{0.65})Fe_2O_4$) and ferroxcube 4E ($NiFe_2O_4$) are drawn. The curves for the other nickel-zinc ferrites (ferroxcube 4B, 4C, 4D) lie between them in the shaded portion. Also drawn in this shaded part is the curve for lithium ferrite ($(Li^{1+}_{0.5}Fe^{3+}_{0.5})Fe^{3+}_2O_4$). All the curves, except that for iron, are continued to near the saturation point. For the ferroxcube 4 materials the saturation points lie on the dotted boundary line of the shaded portion. The value of ε at saturation, i.e. the saturation magnetostriction ε_s, can be found in *Table I* and is a measure of the suitability of a material for high-power piezomagnetic radiators. For metals and alloys ε_s varies from 70×10^{-6} ("2V-Permendur") to -33×10^{-6} (Ni), and for ferrites from 40×10^{-6} (ferrous ferrite) to -27×10^{-6} (nickel ferrite). The permanently magnetic materials cobalt and cobalt ferrite are not taken into account here (although $CoFe_2O_4$ does appear in the table).

Additional data given in the table, besides ε_s and the saturation polarization J_s ($\approx$ saturation induction B_s), are: the D.C. electrical resistivity ϱ_{el}, the Curie temperature T_c, and the coupling coefficient at remanence k_{rem}. A high Curie temperature is of interest if the material is to be used at high temperatures. Disregarding "Permendur" which has a very high T_c and ferroxcube 4A which has a very low T_c, it will be seen that in this respect the ferrites are comparable with alloys. We shall come back to the significance of the coupling coefficient later.

In fig. 1 no account is taken of hysteresis. The figure holds for materials which are in the virgin state when the (macroscopic) induction is zero. In *fig. 2a* the general relationship between B and H is represented schematically; both the virgin curve and the hysteresis loop are shown. In fig. 2*b* the corresponding relationship between ε and H is given. The sign of the magnetostriction is independent of the sign of H, hence a butterfly-shaped curve is obtained. Fig. 2*c* shows the roughly quadratic relationship between ε and B.

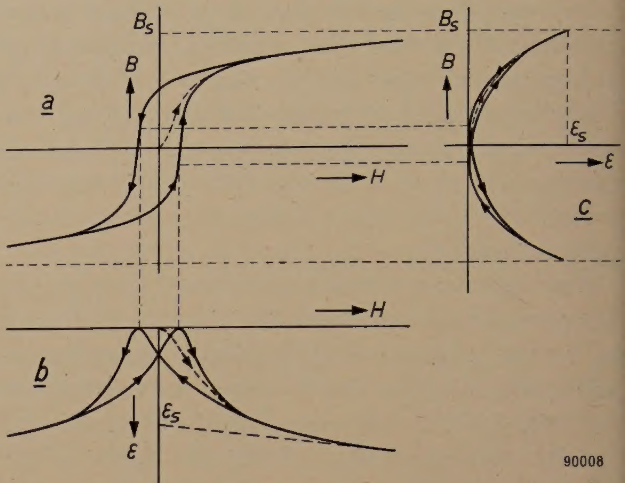

Fig. 2. *a*) B as a function of H; *b*) ε as a function of H; *c*) ε as a function of B. Both the hysteresis loops and the virgin curves are drawn (static behaviour).

If, starting from a point on the virgin curve, H is allowed to decrease slightly and then to increase (see *fig. 3*), a narrow loop is described in the B-H diagram. The slope of this loop corresponds to the "reversible permeability". A similar loop is described in the ε-H diagram. It is assumed that there is no

Table I. Properties of various materials for piezomagnetic vibrators. For the ferrites the molecular composition is indicated; for the alloys the composition is quoted in percentages by weight. The porosity p, on which the saturation polarization J_s of the ferrites depends, is defined as pore volume/total volume.

Material	Composition	$10^6\ \varepsilon_s$	J_s (Wb/m²)	ϱ_{el} (Ωm)	T_c (°C)	$\lvert k_{rem}\rvert$
"2V-Permendur"	2 V, 49 Co, 49 Fe	+ 70	2.4	$2.5\text{-}4 \times 10^{-7}$	980	0.19 - 0.26*)
"13 Alfer"	13 Al, 87 Fe	+ 40	1.3	9×10^{-7}	~ 500	0.19 - 0.26*)
"45 Permalloy"	45 Ni, 55 Fe	+ 27	1.6	$5\text{-}7 \times 10^{-7}$	~ 440	0.11 - 0.17*)
Nickel	99.9 Ni	— 33	0.63	0.7×10^{-7}	358	0.14 - 0.23*)†)
Nickel-cobalt alloy	96 Ni, 4 Co	— 31	0.68	1.0×10^{-7}	410	0.34*)†)
Ferrous ferrite	$Fe^{2+}Fe^{3+}_2O_4$	+ 40	0.61 (1—p)	~ 10^{-4}	580	—
Ferroxcube 4A	$Ni^{2+}_{0.35}Zn^{2+}_{0.65}Fe^{3+}_2O_4$	— 5	0.40 (1—p)	$\geqq 10^4$	190	0.06 - 0.10**)
Lithium ferrite	$(Li^{1+}_{0.5}Fe^{3+}_{0.5})Fe^{3+}_2O_4$	— 8	0.39 (1—p)	$\geqq 10^4$	640	0.03 - 0.05**)
Ferroxcube 4E	$Ni^{2+}Fe^{3+}_2O_4$	— 27	0.33 (1—p)	$\geqq 10^4$	590	0.14 - 0.20**)
Nickel-cobalt ferrite	$Ni^{2+}_{0.98}Co^{2+}_{0.02}Fe^{3+}_2O_4$	— 26	0.33 (1—p)	$\geqq 10^4$	590	0.22 - 0.25**)
Cobalt ferrite	$Co^{2+}Fe^{3+}_2O_4$	~ —200	0.54 (1—p)	$\geqq 10^4$	510	—

*) Dependent on the mechanical and thermal treatment of the laminations.

**) Dependent on the porosity, i.e. the sintering temperature. The high value reported is that found for a certain optimum porosity (p_1 in Table II). The low values reported for ferroxcube 4A and 4E are those of the currently available commercial materials, for which the porosity p is given in Table II.

†) C. A. Clark, The dynamic magnetostriction of nickel-cobalt alloys, Brit. J. appl. Phys. 7, 355-360, 1956.

external tensile stress σ acting on the rod during these variations in B and ε. The slopes of the loops are therefore designated by $(\partial B/\partial H)_\sigma = \mu^\sigma$ and $(\partial \varepsilon/\partial H)_\sigma = d$ respectively [9]). It is also possible to vary H and at the same time to subject the rod, for example by clamping it, to such forces that no change in length ε can occur. A different value is then obtained for the permeability which we designate by $(\partial B/\partial H)_\varepsilon = \mu^\varepsilon$. Piezomagnetic behaviour manifests itself in the fact that μ^σ and μ^ε have different values, i.e. $\mu^\sigma > \mu^\varepsilon$. If, starting from a state in which $B = B_0$, $H = H_0$, we subject the rod to an alternating magnetic field with amplitude $\hat{H}$, then for the unclamped rod the maximum magnetic energy is $\frac{1}{2}\mu^\sigma \hat{H}^2$ and for the clamped rod only $\frac{1}{2}\mu^\varepsilon \hat{H}^2$. In the first case, however, internal elastic energy is supplied to a value of $\frac{1}{2}(\mu^\sigma - \mu^\varepsilon)\hat{H}^2$. As can be seen from the above, the ratio

$$k^2 = \frac{\mu^\sigma - \mu^\varepsilon}{\mu^\sigma} \quad \ldots\ldots \quad (1)$$

gives the fraction of the magnetic energy which can be converted into mechanical energy. The root of this quantity, i.e. k, is the magnetomechanical or piezomagnetic coupling coefficient reported in Table I. For ferrites k^2 may have a value up to 0.10.

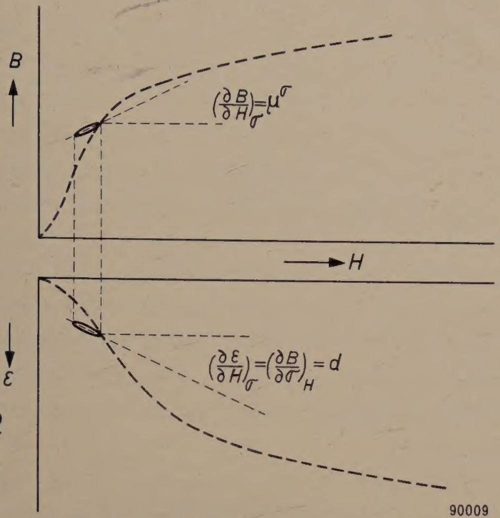
B
a
$(\frac{\partial B}{\partial H})_\sigma = \mu^\sigma$
H
ε
b
$(\frac{\partial \varepsilon}{\partial H})_\sigma = (\frac{\partial B}{\partial \sigma})_H = d$
90009

Fig. 3. Dynamic behaviour of B and ε as functions of H, for normal piezomagnetic material.

The quantity k^2 must be clearly distinguished from the electroacoustic efficiency η_{ea} to be discussed later (the latter is the percentage of the electrical power supplied that is converted into acoustic power) which can attain values of almost 100%.

The rod can, of course, also be subjected to an alternating tensile stress without being subjected to a magnetic field. The specific elastic compliance can be determined in this way. Since the determination is carried out with H constant, the compliance found is designated by $(\partial \varepsilon/\partial \sigma)_H = 1/E^H$. If the rod thus strained is in the virgin state ($H_0 = 0$, $B_0 = 0$), no magnetic changes are perceptible. The macroscopic induction is and remains zero. If, however, the rod is initially in a magnetized state ($B_0 \neq 0$), the extension results in a change of induction. The quantity in question $(\partial B/\partial \sigma)_H$ is found to equal the quantity $(\partial \varepsilon/\partial H)_\sigma$ discussed above, so that $(\partial B/\partial \sigma)_H$ is likewise equal to d. If it is required to suppress any change in induction brought about by the strain, the rod must be surrounded by a short-circuited solenoid having zero resistance. Currents will then be set up in the turns of this coil, so as to keep B constant. The resulting compliance $(\partial \varepsilon/\partial \sigma)_B = 1/E^B$ differs from the compliance $1/E^H$ just discussed, and in fact $1/E^H > 1/E^B$. It is also found that

$$k^2 = \frac{1/E^H - 1/E^B}{1/E^H} \quad \ldots\ldots \quad (2)$$

Because magnetic and elastic losses occur with alternating magnetic and mechanical loading, the

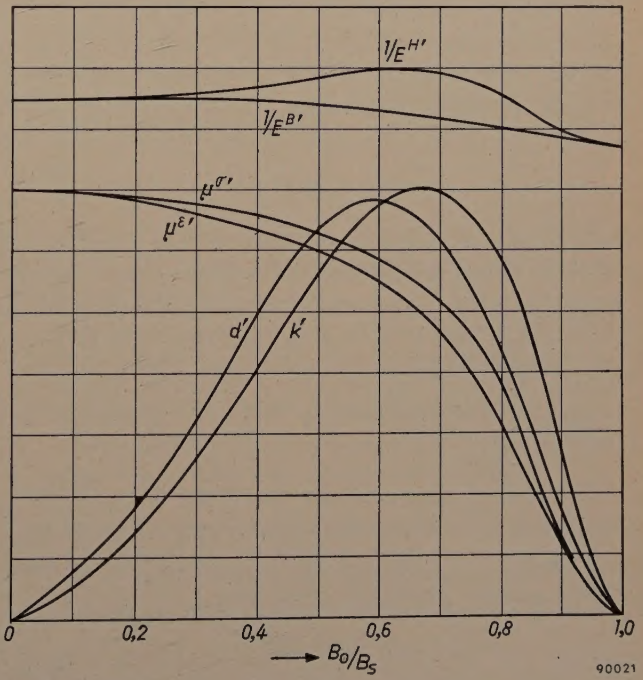

Fig. 4. Schematic curves for $\mu^{\sigma'}$, $\mu^{\varepsilon'}$, $1/E^{H'}$ and $1/E^{B'}$ together with the sensitivity constant d' and the coupling coefficient k', as functions of B_0/B_s, for a ferroxcube. Virgin curves, i.e. the curves for the reversible dynamic constants shown hold for working points on the virgin curve of increasing magnetic bias.

---

[9]) Following the standardized system adopted in the U.S.A. for the analogous piezoelectric case (Proc. Inst. Radio Engrs. **37**, 1378-1395, 1949), we print the variable which is kept equal to zero or, in the general case, is kept constant, as a superscript and not as a subscript of the quantities μ and E (permeability and modulus of elasticity).

quantities μ^σ, μ^ε, $1/E^H$ and $1/E^B$ are complex [10]. In *fig. 4* the real parts $\mu^{\sigma'}$, $\mu^{\varepsilon'}$, $1/E^{H'}$ and $1/E^{B'}$ of these quantities as well as the real parts d' and k' of d and k are plotted as functions of B_0/B_s.

The behaviour of piezomagnetic vibrators in the resonance band

The two main forms of piezomagnetic vibrators are the rod vibrator and the ring vibrator, consisting respectively of a rod or ring-shaped core made of a piezomagnetic material and surrounded by a coil. Like any other solid body the core can perform free elastic vibrations having a number of modes of vibration and corresponding characteristic frequencies. We shall confine ourselves to the fundamental frequency. The fundamental frequency of the rod on open circuit (i.e. in the absence of an alternating magnetic field) corresponds to a longitudinal vibration with a displacement node (strain antinode) at the centre and displacement antinodes (strain nodes) at either end. The length l of the rod corresponds to half a wavelength. Since the product of frequency and wavelength is equal to the velocity of sound $v^H = (E^{H'}/\varrho)^{1/2}$ in the material, the frequency of free vibration is given by

$$f^H = \frac{1}{2l}\left(\frac{E^{H'}}{\varrho}\right)^{\frac{1}{2}}, \quad . \quad . \quad . \quad . \quad (3a)$$

where ϱ is the specific gravity.

In the case of the ring the fundamental frequency corresponds to a mode of vibration in which the circular shape is preserved, but the diameter $2R$ is a periodic function of the time. For the ring we have

$$f^H = \frac{1}{2\pi R}\left(\frac{E^{H'}}{\varrho}\right)^{\frac{1}{2}}. \quad . \quad . \quad . \quad . \quad (3b)$$

For formula (3a) we must not use for $E^{H'}$ the value discussed above, which we find for homogeneous strain, but an average value which is somewhat higher than $E^{H'}$. The reason for this is connected with the fact that the alternating induction along a half-wave vibrator may be practically constant, whereas the alternating strain is a sinusoidal function of position, as in the window-type half-wave vibrator to be discussed in the next section.

The rod or ring can also be allowed to vibrate elastically with the coil short-circuited. This being the case, B is constant and $v^B = (E^{B'}/\varrho)^{1/2}$. The corresponding vibration frequency is

$$f^B = \frac{1}{2l}\left(\frac{E^{B'}}{\varrho}\right)^{\frac{1}{2}} \quad . \quad . \quad . \quad . \quad . \quad (4a)$$

for the rod, and

$$f^B = \frac{1}{2\pi R}\left(\frac{E^{B'}}{\varrho}\right)^{\frac{1}{2}} \quad . \quad . \quad . \quad . \quad (4b)$$

for the ring. The frequencies f^H and f^B lie close together, and

$$\frac{f^B - f^H}{f^B} \approx \tfrac{1}{2}|k^2|/\varphi, \quad . \quad . \quad . \quad . \quad (5)$$

where $\varphi \approx \pi^2/8$ for the rod and $\varphi = 1$ for the ring.

If an alternating current is passed through the coil, then owing to the piezomagnetic effect, the length of the polarized rod or the diameter of the polarized ring (as the case may be), will be a periodic function of the time. The rod or the ring then performs forced vibrations whose amplitude in the resonance band may be large compared with their amplitude outside this band, as a result of the high mechanical Q.

The behaviour in the resonance band can be investigated by measuring the impedance Z or the admittance $Y\,(= Z^{-1})$ as a function of the frequency. In *fig. 5* the absolute values $|Z|$ and $|Y|$ are plotted as functions of f. It will be seen that $|Z|$ has a maximum at frequency f_{r} ("resonance frequency") and a minimum at frequency f_{a} ("anti-resonance frequency"). For $|Y|$, of course, the maximum and minimum are interchanged. If the maximum value of $|Z|$ is many times greater than the value of $|Z|$ outside resonance (say at least 10 times), then to a very close approximation $f_{\mathrm{r}} = f^H$ and $f_{\mathrm{a}} = f^B$. Consequently between f_{r} and f_{a} there likewise exists the relationship

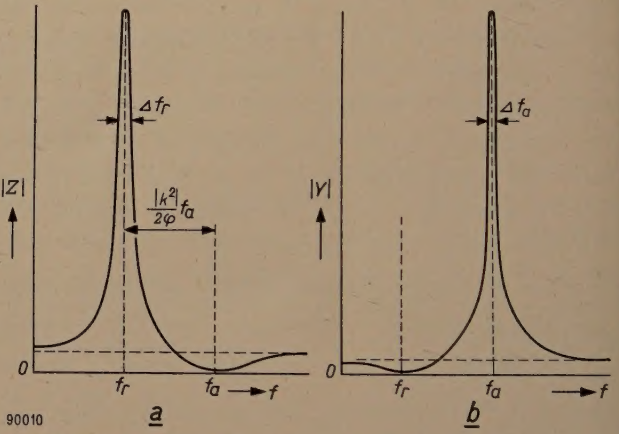

Fig. 5. Absolute values for the impedance Z and the admittance Y of a ferroxcube vibrator (in air), as functions of the frequency f. Here $f_{\mathrm{a}} - f_{\mathrm{r}} \approx f^B - f^H \approx \frac{1}{2}(|k|^2/\varphi)f^B$, where $\varphi = 1$ for ring vibrators and $\varphi \approx \pi^2/8$ for half-wave vibrators. At anti-resonance the mechanical $Q(= f/\Delta f)$ is considerably higher than at resonance.

$$\frac{f_{\mathrm{a}} - f_{\mathrm{r}}}{f_{\mathrm{a}}} \approx \tfrac{1}{2}|k^2|/\varphi. \quad . \quad . \quad . \quad . \quad . \quad (6)$$

---

[10] They are therefore of the form $a = a' - \mathrm{j}a'' = a'(1 - \mathrm{j}\delta)$, where a'' is always much smaller than a' and consequently the loss angle $\delta \ll 1$. Further $|a| = \sqrt{a'^2 + a''^2} \approx a'$. The mechanical Q and magnetic Q later to be discussed are defined by $Q = 1/\delta$.

The above refers to a non-radiating vibrator, i.e. when it is vibrating in air (the radiation is then negligible) or in vacuum, and when the coil is so mounted that the core can vibrate without touching it. If the vibrator is in contact with a liquid, acoustic waves are launched into the latter, and the vibrator is strongly damped. Intimate contact between vibrator core and coil and in the case of a laminated core, friction between the laminations can also contribute to the damping.

Since a liquid in contact with the radiating surface of the vibrator will move with the latter, the apparent mass of the vibrator will increase, at least, if no plane acoustic waves are launched. As a result the resonance frequencies will be shifted, becoming somewhat lower. Simultaneously, damping will flatten and broaden the maxima of $|Z|$ and $|Y|$.

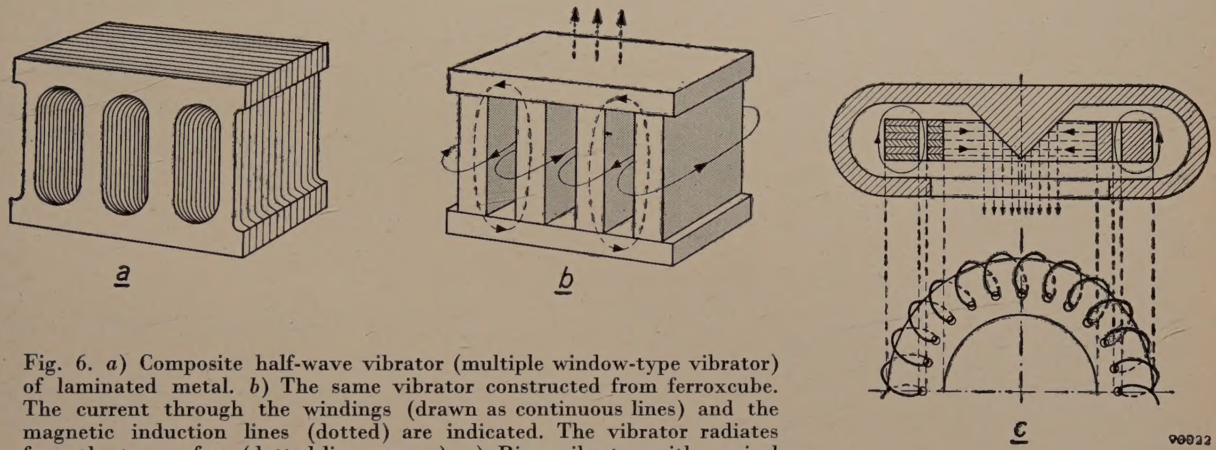

Fig. 6. *a*) Composite half-wave vibrator (multiple window-type vibrator) of laminated metal. *b*) The same vibrator constructed from ferroxcube. The current through the windings (drawn as continuous lines) and the magnetic induction lines (dotted) are indicated. The vibrator radiates from the top surface (dotted-line arrows). *c*) Ring vibrator with conical reflector; to show how the metal construction would appear, lamination of the ring is drawn on the left of the centre line. The direction of radiation is indicated by dotted-line arrows. Radiation from the surface opposite and parallel to the radiating surface is prevented by a sheet of acoustic shielding material such as cell-tight foam rubber.

Damping leads moreover to the dissipation of power of which only the radiated power is useful. The other types of dissipation (magnetic and elastic) must be regarded as losses, and give rise to heating of the vibrator core and coil.

Some conventional forms of piezomagnetic transducers

The ring and rod vibrators discussed above are actually employed in practice. Rod vibrators are often in the form of several rods or plates arranged alongside each other and connected together by means of end plates (window-type vibrators). In *fig. 6* piezomagnetic transducers such as are used at frequencies of about 30 kc/s, are shown schematically.

Fig. 6*a* represents a half-wave radiator of piezomagnetic metal, showing the laminations. The latter are about 0.1 - 0.2 mm thick for nickel and about 0.2 - 0.4 mm thick for "Alfer" and "Permendur".

Fig. 6*b* represents a corresponding ferroxcube vibrator. The core is not laminated. The legs are of strongly piezomagnetic ferroxcube (e.g. nickel-cobalt ferrite). The end plates are made of non-piezomagnetic or weakly piezomagnetic material having a high saturation polarization (e.g. manganese-zinc ferrite or nickel-zinc ferrite). To ensure linearity the core is given a biasing polarization as described in the introduction. This polarization (which may be remanent polarization) is parallel to that of the alternating induction (indicated in the figure).

To avoid the necessity of a strong direct current for the biasing of high-intensity radiators, one may instead cement in each magnetic circuit one or two thin slices of permanent-magnet ceramic material [11]), for example ferroxdure [12]).

In fig. 6*c* a "breathing" ring vibrator with reflector is shown (constructed in laminated metal or ferroxcube). The turns are led through holes in the ring so that the radiating surface (here the inside surface) is left free. Ring vibrators also exist in which radiation takes place from the outside surface.

Fig. 7 is a photograph of a ferroxcube half-wave transducer with and without windings.

The generation of acoustic waves

The most important quantities involved in the generation of acoustic waves in a medium are: the

---

[11]) Y. Kikuchi and co-workers, Magnetostrictive ultrasonic transducers made of ferrites, Sci. Rep. Res. Insts. Tôhoku Univ. (B) 7, 9-15, 1955.

[12]) J. J. Went, G. W. Rathenau, E. W. Gorter and G. W. van Oosterhout, Ferroxdure, a class of new permanent magnet materials, Philips tech. Rev. **13**, 194-208, 1951/52. See also an article by H. G. Bruijning and A. Rademakers, to appear shortly in this Review.

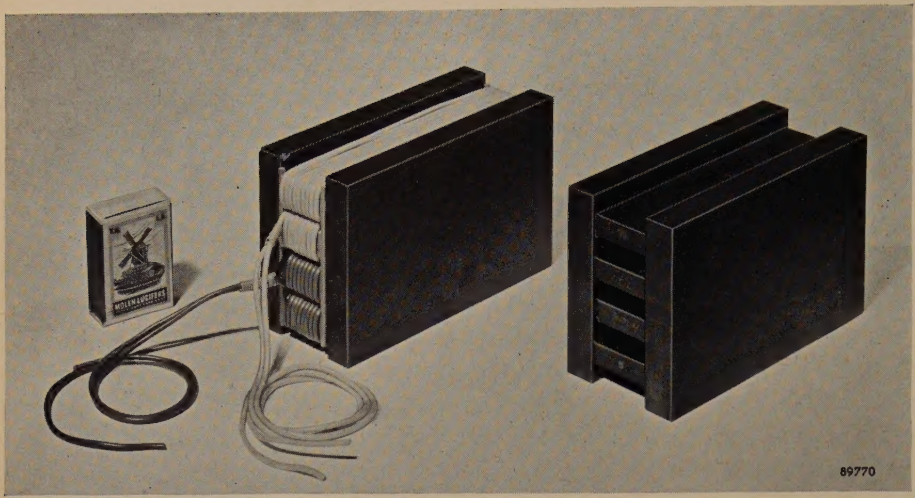

Fig. 7. A photograph of a ferroxcube half-wave transducer (multiple window type), with windings and without.

electroacoustic efficiency η_{ea} and the maximum acoustic power radiated.

The energy consumed is the sum of all the dissipations. The electroacoustic efficiency is therefore:

$$\eta_{\mathrm{ea}} = \frac{\text{dissipation by radiation}}{\text{sum of all dissipations}} . \quad (7)$$

A high efficiency is desirable in ferroxcube vibrators, not so much because of power consumption as because of the fact that dissipation of energy in the vibrator leads to heating of the vibrator core and hence to thermal stresses. Owing to the brittleness of the material this would lower the maximum permissible alternating strain and consequently the maximum safe intensity. We shall return to this point a little later.

The maximum electroacoustic efficiency

For a given vibrator the values of the losses and of the dissipation by radiation, hence also of η_{ea}, depend upon the frequency of the alternating magnetic field.

In *fig. 8b* the electric power supplied, at almost constant voltage ($\hat{V} \propto f^{\frac{1}{2}}$), is plotted as a function of the frequency. As fig. 8*a* shows, this power can be derived from the complex diagram for the quantity fY (Y = the admittance of the vibrator), which is proportional to $1/\mu$ (where μ is the complex permeability of the vibrator). In fig. 8*a* and *b* the state of affairs is shown with the vibrator in air and in water.

It is now found that, if the copper losses can be ignored, the highest value for η_{ea} is obtained when the vibrator is operated at the frequency f_{max} ($\approx f^B \approx f_{\mathrm{a}}$) at which the real part $\mathrm{Re}(fY)$ is a maximum [13] [14]). In what follows we shall assume that this is always the case. We then have [15]):

$$\eta_{\mathrm{ea\,max}} = \frac{D_{\mathrm{W}}}{h + D_{\mathrm{W}}} \, \frac{D_{\mathrm{V}} - D_{\mathrm{W}}}{D_{\mathrm{V}}} . \quad (8)$$

We shall not go into the derivation of this formula here. (This will be discussed in a second article to appear in this Review.) D_{V} and D_{W} are the diameters of the admittance circles (fig. 8*a*) when the completely assembled vibrator is set up in air (or in vacuum) and in water respectively; h is the smallest distance from the admittance circles to the imaginary axis (see fig. 8*b*). D_{V} and D_{W} are proportional to $|k^2|$; further D_{V} is proportional to the mechanical Q in air (see [10])), and h is inversely proportional to the magnetic Q. Hence, $\eta_{\mathrm{ea\,max}}$ increases with increasing mechanical and magnetic Q's and with increasing k.

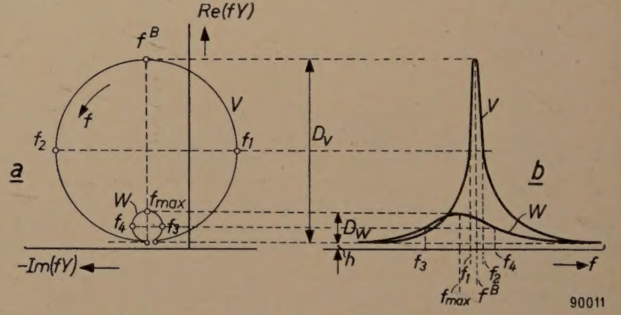

Fig. 8. *a*) Complex diagram of fY with f as parameter, for a vibrator in air or vacuum (V) and in water (W). In reality the ratio of the diameters of the two circles is between 10 and 100. *b*) The real part $\mathrm{Re}(fY)$ as a function of f. For an approximately constant voltage ($\hat{V} \propto f^{1/2}$), $\mathrm{Re}(fY)$ is proportional to the electrical power supplied to the vibrator.

If we compare vibrators of different dimensions, whose working frequencies ($= f_{\mathrm{max}}$) will therefore also be different, then $\eta_{\mathrm{ea\,max}}$ can be plotted as a function of this frequency. In addition $\eta_{\mathrm{ea\,max}}$ will depend upon the shape of the vibrator and on the nature of the piezomagnetic material, and also, to a small extent, on the power radiated. In *fig. 9*, $\eta_{\mathrm{ea\,max}}$ is plotted roughly as a function of f_{max} for window-type radiators. The curves given refer to laminated metallic materials, at a radiation intensity of 0.5 to 5 W/cm², and to suitable types of ferroxcube, at intensities < 2 W/cm² and > 2 W/cm². It can be seen that even for such low frequencies as 20 kc/s, ferroxcube is preferable to metal. The superiority of ferroxcube is due to the absence of eddy-current losses and frictional losses between laminations.

---

[13]) Y. Kikuchi and H. Shimizu, On the "B-type" resonance of magnetostriction and electrostriction transducers, Sci. Rep. Res. Insts. Tôhoku Univ. (B) 4, 173-203, 1952.

[14]) H. Thiede, Untersuchungen an Ferriten auf ihre Eignung als Flüssigkeitsschallwandler, Acustica 4, 532-536, 1954; see also page 122 et seq. of the book by Hunt cited in note [4]).

[15]) Design and construction of magnetostriction transducers, Summary Technical Report, Div. 6, NDRC, Vol. 13, Washington (D.C.) 1946, page 59 (PB Report No. 77 669).

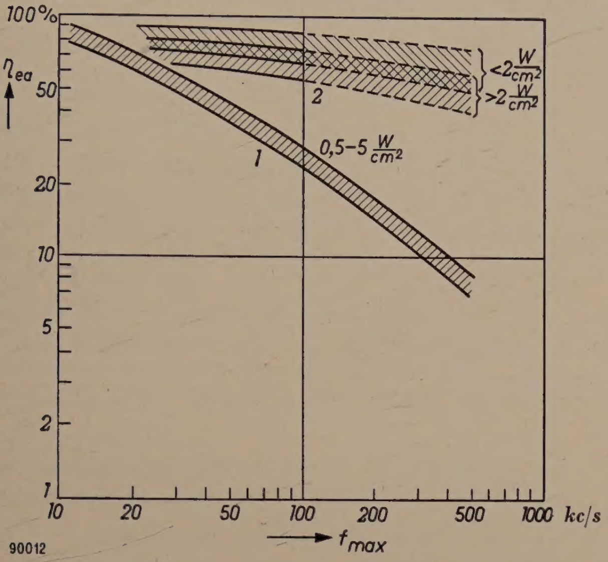

Fig. 9. Electroacoustic efficiency η_{ea} for vibrators in continuous operation (working constantly at their optimum frequency f_{max}) as a function of f_{max}; curves *1* for metals, 0.5-5 W/cm² (data from the literature), curves *2* for ferroxcube, <2W/cm² and >2W/cm² (very few measurements have been made above 100 kc/s).

The maximum safe load of ferroxcube radiators

A second important point in the generation of acoustic waves is the maximum safe load. This is determined by the mechanical strength of the material, for during vibration it is subjected in turn to tension and compression. Now, it is well known that the ultimate unidirectional compressive stress of ceramic materials exceeds their ultimate tensile stress by a factor of 10-30, so that the tensile strength is the determining quantity. An idea of the magnitude of the tensile strength can be obtained from easily performed bending tests. The tensile strength, the bending strength and the compressive strength all fall as the porosity p (pore volume/total volume) increases. This can be seen from *fig. 10* in which the compressive strength and the tensile strength (the latter from bending and tensile tests) of ferroxcube 4 materials are plotted as functions of p. It will be noted that the tensile strength calculated from bending tests is somewhat too high for dense ferrites and somewhat too low for porous ferrites, compared with the tensile strength found in very carefully performed tensile tests. When using these data it must also be taken into account that the tensile strength of ceramic materials is a function of the cross-sectional area — or better, of the volume — of the material, since the fracture in ceramic materials is essentially a matter of statistics. Fracture is initiated at the weakest point in the volume under load: the probability of there being a weak point increases as the volume increases. There are various indications that the tensile strength, as reported in fig. 10, should be divided by a factor of 2 to 3 for very large cross-sections in order to obtain the correct value. The experimental curves given in fig. 10 refer to cross-sections of 2 mm × 3 mm.

It has been found in practice [16]) that even rods of ferroxcube 4D (length 6 cm, cross-section 2 cm²), which has not been specially prepared for piezomagnetic applications and having (in this respect) an unfavourably high porosity ($p = 0.20$), can continuously deliver an intensity of 8 W/cm² at 40 kc/s from both ends with an efficiency greater than 0.7.

It can be safely assumed that if the material is judiciously chosen (good homogeneity, small p and large k, and hence a large $\eta_{\mathrm{ea\,max}}$), it will be possible to obtain continuous radiation intensities of at least 10 W/cm² at 50 kc/s without any great risk of fracture. Systematic tests on this score are still in progress. It can be taken as a rule of thumb that the

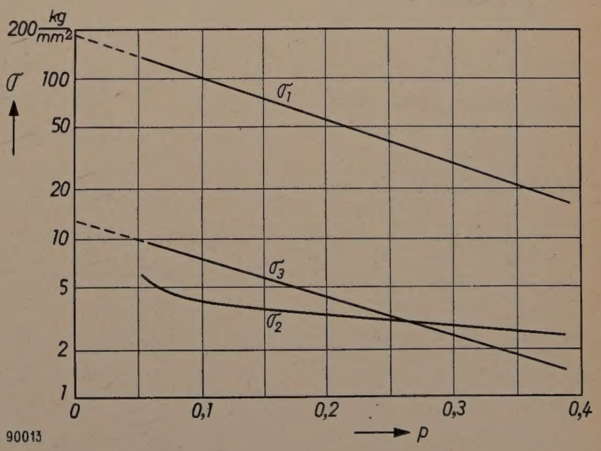

Fig. 10. The compressive strength (σ_1) and the tensile strength from tensile tests (σ_2) and bending tests (σ_3) as functions of the porosity p. The curves are roughly the same for the various types of ferroxcube. All refer to a cross-section of 2 mm × 3 mm.

---

[16]) U. Enz, Erzeugung von Ultraschall mit Ferriten, Dissertation E.T.H. Zürich 1955 (page 45).

maximum safe intensity for continuous loading (C.W. operation) is $15(1-2p)$ W/cm^2.

The figures quoted for the radiation intensity in W/cm^2 refer to simple half-wave bar-type radiators. The area involved is then simply the cross-sectional area of the bar. For window-type radiators the values quoted should be divided by roughly 1.5 (for single window types) or by 1.5 - 2 (for multiple window types), in order to find the values per square centimetre of the *radiating* surface.

Intensities of that magnitude are perfectly satisfactory for many practical applications. If instead of continuous loading, the vibrator is pulse-operated (whereby temperature gradients and hence thermal stresses in the material are avoided), ferroxcube radiators can be expected to give safe radiation intensities of 15 to 20 W/cm^2 in water.

Types of ferroxcube suitable for ultrasonic radiators

We have already seen that the porosity of the ceramic radiators constitutes a limiting factor with respect to the maximum safe intensity. It will however be clear that one should first ensure that the amplitude of the piezomagnetic deformation of the material for reasonable alternating magnetic fields is such that the fracture limit is indeed the determining factor. In practice this means that a strain amplitude $\hat{\varepsilon} = 10^{-4}$ must occur at resonance. If we suppose that outside resonance a strain amplitude of up to about one third of the saturation magnetostriction ε_s may be produced in the premagnetized vibrator by a reasonable field strength, we find that on account of the mechanical Q (in water) of 15-45, $|\varepsilon_s|$ must be equal to or greater than 10×10^{-6}.

Ferroxcube materials of the types thus far available on the market are prepared with special regard to optimum properties for specific magnetic applications. It is hardly surprising, therefore, that they do not at the same time possess the most favourable properties for piezomagnetic applications.

Thus, for example, the commercial materials with the highest values of the saturation magnetostriction are very porous (see *Table II*), and consequently their maximum safe intensity and their piezomagnetic coupling are lower than would be the case for denser specimens. *Fig. 11c* shows the improvement in the coupling coefficient at remanence which is obtained by giving the materials the most favourable densities by special methods of preparation (e.g. higher sintering temperature). The coupling coefficient at remanence can be given still higher values by introducing slight changes in the chemical composition, namely by adding cobalt; we shall return to this point in the last section.

Table II. Saturation magnetostriction (ε_s), Curie temperature (T_c) *) and saturation polarization (J_s) of nickel-zinc ferrites ($Ni_{1-y}Zn_yFe_2O_4$). Column 5 lists the corresponding commercial ferroxcubes, the approximate porosities of which are given under p; the desired approximate porosities for maximum values of $|k_{rem}|$ are given under p_1. When the material is completely free from pores its specific gravity is about 5.35 g/cm^3.

y	$10^6\varepsilon_s$	T_c (°C)	J_s (Wb/m^2)	Type of ferroxcube	p	p_1
0	−27	590	0.33 (1−p)	4E	0.25	0.12
0.20	−21	490	0.47 (1−p)	4D	0.20	0.09
0.35	−16	400	0.52 (1−p)	4C	0.15	0.07
0.50	−11	290	0.49 (1−p)	4B	0.11	0.06
0.65	− 5	190	0.40 (1−p)	4A	0.08	0.05

*) By Curie temperature is understood the temperature at which the saturation polarization becomes roughly zero, and not the temperature at which μ sharply falls.

These improved materials will be put on the market as soon as demand for them warrants their production in reasonably large quantities.

In many cases, e.g. for high radiation intensities, it is not so much the highest possible value of the coupling coefficient at remanence that is required, as the highest possible value of $|k|$ at the optimum biasing polarization, $J_0 \approx 0.7\ J_s$ (see fig. 4). The tensile strength should likewise be as large as

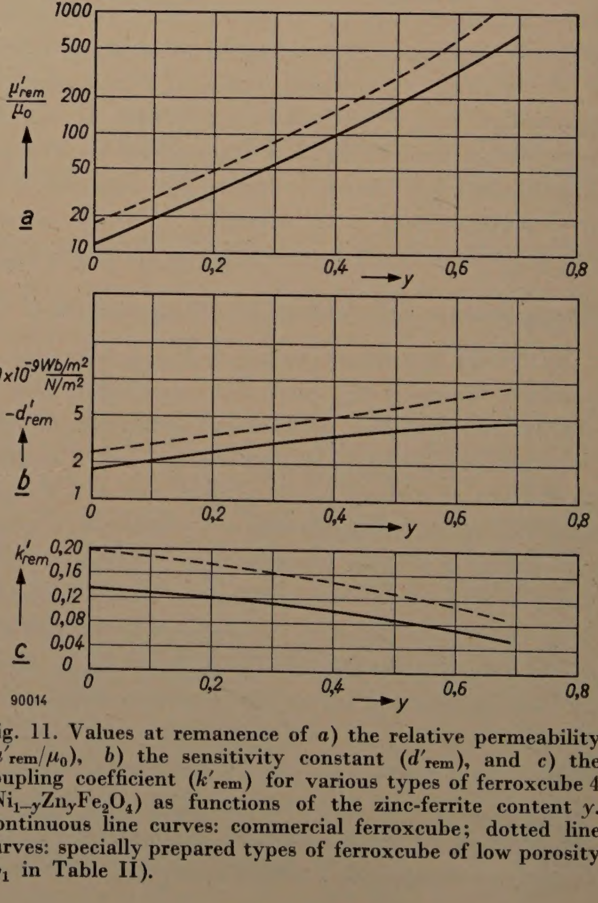

Fig. 11. Values at remanence of *a*) the relative permeability (μ'_{rem}/μ_0), *b*) the sensitivity constant (d'_{rem}), and *c*) the coupling coefficient (k'_{rem}) for various types of ferroxcube 4 ($Ni_{1-y}Zn_yFe_2O_4$) as functions of the zinc-ferrite content y. Continuous line curves: commercial ferroxcube; dotted line curves: specially prepared types of ferroxcube of low porosity (p_1 in Table II).

possible. Both requirements call for the highest attainable density of the ferrite; high density can be imparted either by carrying out the sintering process at a very high temperature or by replacing part of the nickel (and zinc) by copper [17]).

The detection of acoustic waves

The half-wave window-type vibrators and ring vibrators shown in fig. 6, are also used for detecting acoustic waves. Another much-used form is the cylindrical receiver which may be regarded as a ring whose height is large compared with the diameter. This receiver is characterized by a sharp directivity pattern over a wide frequency range.

If it is required to receive a single frequency, the mechanical resonance frequency of the receiver must be made to coincide with that frequency. If a broad frequency band is to be detected, the resonance frequency is made higher than the highest frequency to be received, since then the frequency response is not so strongly dependent upon the frequency ($\propto f$).

An important quantity in detection is $(\partial B/\partial \sigma)_H = d$ introduced above, which determines the change in induction in the material brought about by an external stress. d is usually called the "sensitivity constant".

Nevertheless the quantity d does not always determine the sensitivity of the detector. This is connected with the fact that in the NiZn ferrite series (the ferroxcube 4 materials), the permeability μ and likewise, if the number of turns n remains the same, the self-inductance L_W of the windings, increase with increasing d (fig. 11).

The determining quantity is the ratio of the amplitude $\hat{V}$ of the open-circuit voltage to the amplitude $\hat{\sigma}$ of the pressure of the incident wave:

$$\frac{\hat{V}}{\hat{\sigma}} = \frac{\omega n A \hat{B}}{\hat{\sigma}} = \omega n A |d|, \quad . \; . \; . \quad (9)$$

where A is the cross-sectional area.

The vibrational frequency of the circuit, the latter comprising the self-inductance $L = L_W + L_s$ (L_s being the leakage inductance) and the capacitance C_0 of the connecting cable etc.,

$$f_{\mathrm{el}} = \frac{1}{2\pi (LC_0)^{1/2}}, \quad . \; . \; . \; . \; . \quad (10)$$

may not fall below the value of the highest frequency for which (or up to which) the receiver is to be used. This is because at frequencies greater than f_{el} the capacitance C_0 would short-circuit the signal.

If L_s may be ignored, L_W ($\approx L$) may be regarded as given. Since L_W is proportional to the product $n^2\mu$, the latter is fixed, so that n is proportional to $\mu^{-1/2}$. If we ignore the leakage, we find that, according to (9), the sensitivity of the detector is determined by $d/\mu^{1/2}$. This means that we should regard the coupling coefficient

$$k = d(E^H/\mu^\sigma)^{1/2}, \quad . \; . \; . \; . \; . \quad (11)$$

and not d as the determining quantity because E^H, the modulus of elasticity, is roughly the same for all dense NiZn-ferrites.

If L_s becomes a considerable fraction of L, as is the case in long, thin-walled cylindrical receivers (line type hydrophone), we are obliged to select a material for which μ and likewise d are large (see fig. 11). In that case d is more or less the determining constant.

The relative variations of d and k as functions of B_0 have been discussed earlier (see fig. 4). The absolute values of d and k for NiZn ferrites depend upon the zinc content (fig. 11). The latter shows that when k is the determining quantity, nickel ferrite is to be preferred to nickel-zinc ferrites.

For metals, e.g. "Permendur", the coupling coefficient at remanence $|k_{\mathrm{rem}}|$ has a value in the neighbourhood of 0.25. Such values can also be obtained with ferroxcube vibrators if the material is appropriately chosen (see the next section), so that the ferrites likewise bear comparison with metals for the detection of acoustic waves which is frequently done at remanence.

The influence of cobalt on the piezomagnetic properties of ferroxcube

In conclusion we shall discuss the application of ferroxcube filter elements, e.g. for band-pass filters. A band-pass filter may comprise a number of L and C elements and one or more vibrators. An example of such a filter is given in *fig. 12*. The aim of the filter is to pass with negligible attenuation a limited (usually not very narrow) frequency band while largely excluding frequencies outside that band. It is required, moreover, that the edges of the transmission band should be as far as possible unaffected by temperature variations.

The steepness of the edges is connected, amongst other things, with the width of the resonance peaks of the vibrators; that is to say with the mechanical quality factor $Q = f/\Delta f$ (Δf is the interval between the two frequencies for which $|Z|$ and $|Y|$ (fig. 5) fall to very nearly $1/\sqrt{2}$ of their maximum values). Laminated metals suffer from strong mechanical damping (frictional losses between the laminations) and therefore a correspondingly low quality factor Q. They are usually unsuitable for piezomagnetic filter elements. Ferroxcube, on the other hand, which need not be laminated, possesses Q factors which are adequate for this application (between 2000 and 8000).

---

[17]) Y. Kikuchi and co-workers, Study on ferrites for the use in magnetostriction vibrators, Part II. Ni-Cu ferrite, Sci. Rep. Res. Insts. Tôhoku Univ. (B) 7, 171-178, 1955; see also: L. G. Van Uitert, Nickel-copper ferrites for microwave applications, J. appl. Phys. **27**, 723-727, 1956.

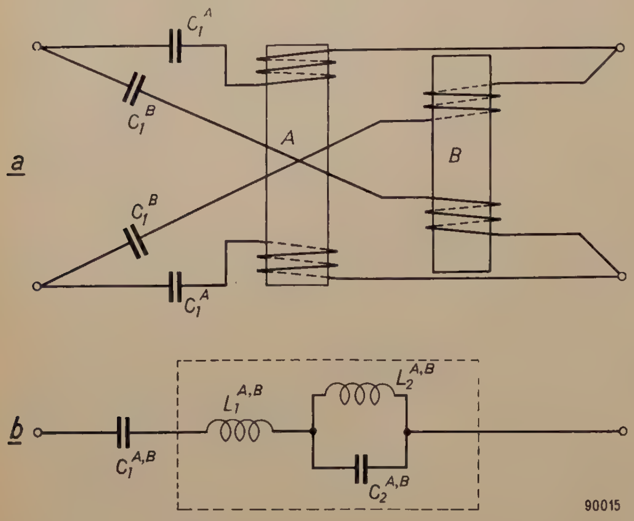

Fig. 12. *a*) Band-pass filter with ferroxcube vibrators. Each of the two cores has two windings. Vibrators *A* and *B* differ slightly and have somewhat different resonance frequencies. (Taken from C.W. Diethelm's "Ferrite als magnetostriktive Resonatoren und deren Anwendung als Elemente elektrischer Filter", Dissertation E. T. H. Zürich 1951; see also Tech. Mitt. PTT **29**, 281-297, 1951.) *b*) Equivalent circuit of one of the branches, magnetic and elastic losses being neglected.

$$L_1 \propto \mu^{s}, \qquad L_2 = \frac{k^2}{1-k^2}\,L_1, \qquad (L_2C_2)^{-1/2} = 2\pi f^H.$$

Temperature variation of the position of the edges is connected with the temperature variation of the anti-resonance frequencies f_a and the resonance frequencies f_r of the vibrators used in the filter and with the temperature variations of the permeability. For normal ferrites f_a and f_r fall off slowly as the temperature increases. The nickel used in the preparation of commercial nickel-zinc ferrites usually contains roughly half a percent of cobalt, so that the variation of f_a and f_r within the temperature range 20-50 °C is normally 0.1-0.25% (increasing with rising zinc content). For cobalt-free ferrites the variation is still greater (roughly 0.3%). All these variations are so large as to preclude the use of these ferrites in filters.

It has been found that the temperature dependence of f_a, f_r, and the permeability of the various ferrites may be considerably altered by adding more cobalt to the ferrite [18] [19]).

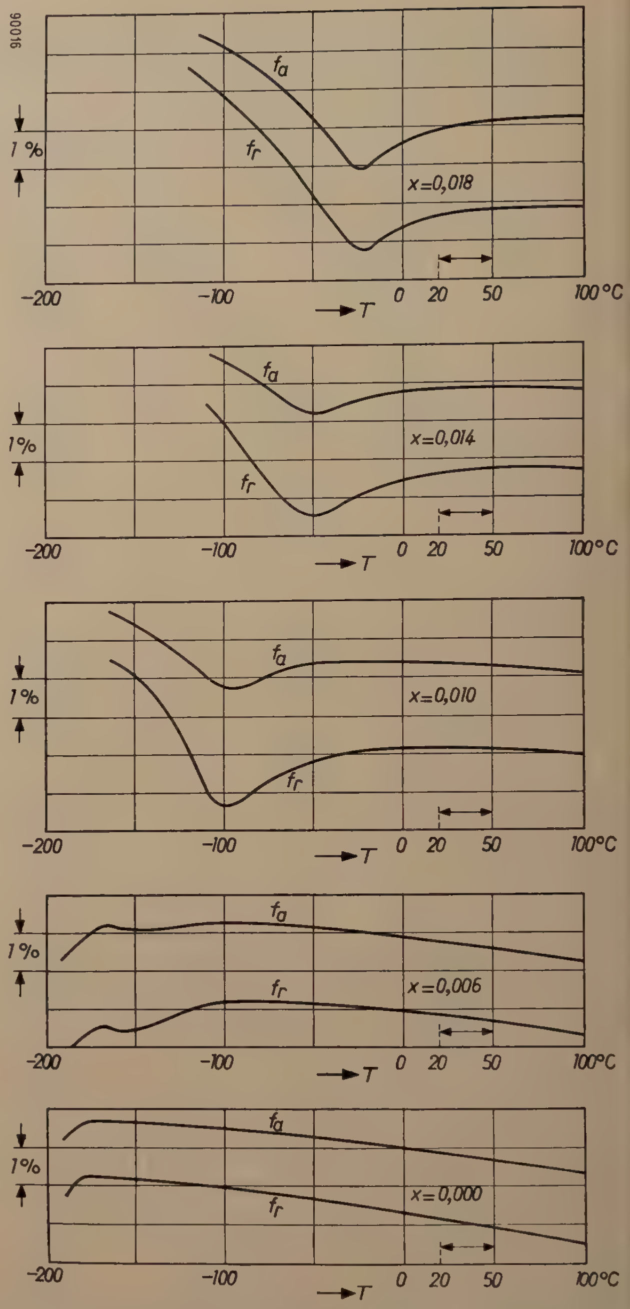

Fig. 13. Behaviour of f_a and f_r (see fig. 5) as functions of temperature for nickel ferrite to which various amounts of cobalt have been added ($Ni_{1-x}Co_xFe_2O_4$). Measurements at remanence.

In *fig. 13* the percentage variations of f_a and f_r at remanence, for nickel-cobalt ferrites ($Ni_{1-x}Co_xFe_2O_4$), are plotted against the temperature; *fig. 14* shows the initial permeability of the same ferrites

---

[18]) C. M. van der Burgt, Ferrites for magnetic and piezomagnetic filter elements with temperature-independent permeability and elasticity, shortly to appear in Proc. Inst. Electr. Engrs. (B) **104**, 1957, Supplement No. 7.

[19]) C. M. van der Burgt, Controlled crystal anisotropy and controlled temperature dependence of the permeability and elasticity of various cobalt-substituted ferrites, shortly to appear in Philips Res. Rep. **12**, 1957.

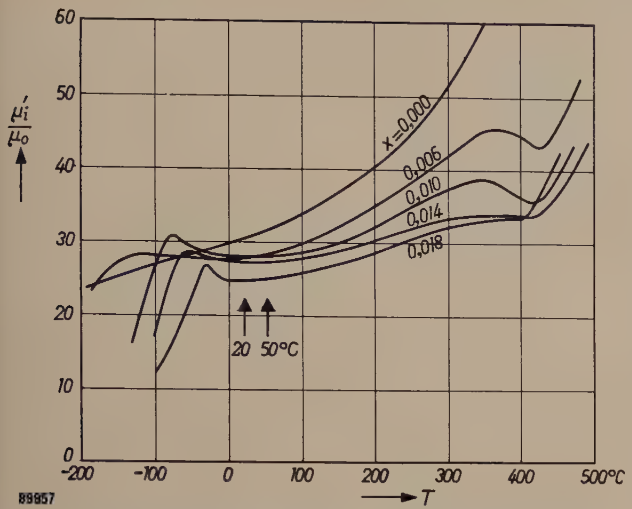

Fig. 14. Behaviour of the relative initial permeability (μ_i'/μ_0) as a function of the temperature for nickel-cobalt ferrites ($Ni_{1-x}Co_xFe_2O_4$).

likewise as a function of temperature. It will be seen that a value for x can be found for which the variations of both f_a and f_r at remanence are less than 0.03% between 20 °C and 50 °C, while the variation of the reversible permeability at remanence is also strongly reduced. This is sufficient in many cases in practice. At a somewhat different value of x the variation of the initial permeability between 20 °C and 50 °C is a minimum.

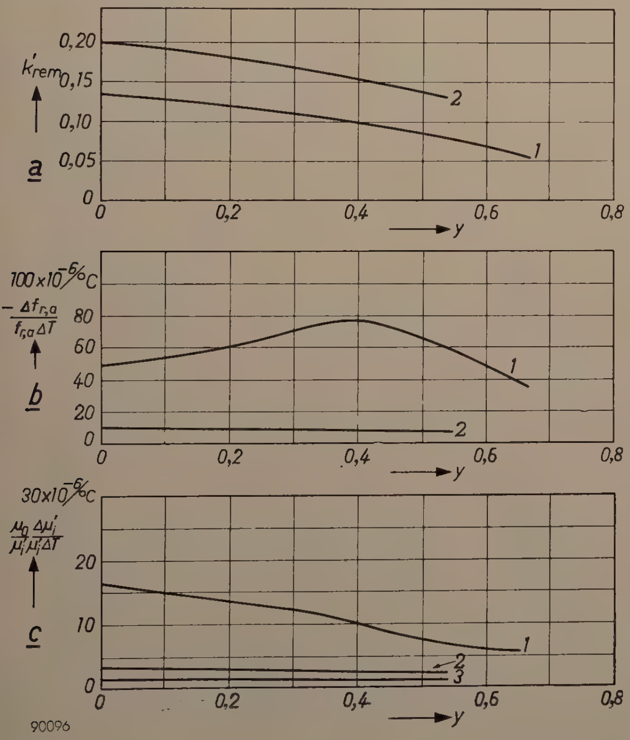

Fig. 15. Improvements in the temperature dependence (*b* and *c*) and the corresponding k'_{rem} (*a*) attained with $(Ni_{1-y}Zn_y)_{1-x}Co_xFe_2O_4$; curves *1* for commercial ferroxcube; *2* for ferroxcube with optimum cobalt content (x) to obtain minimum values of $-(\Delta f_{r,a}/f_{r,a}\Delta T)$ at remanence; *3* as *2* but now with x the optimum value for least temperature dependence of the relative initial permeability μ_i'/μ_0, i.e., for a minimum value of $(\mu_0/\mu_i')(\Delta\mu_i'/\mu_i'\Delta T)$.

A summary of results obtained with ring vibrators of $(Ni_{1-y}Zn_y)_{1-x}Co_xFe_2O_4$ (nickel-zinc-cobalt ferrite) is given in *fig. 15*.

The addition of cobalt likewise favours a high coupling coefficient. In *fig. 16* the coupling coefficients for nickel-cobalt ferrites at remanence are plotted against the temperature. The figure shows that if the primary concern is for a large value of k at room temperature (under-water receivers and radiators), rather than for extreme temperature independence, nickel-cobalt ferrites can be prepared with a value of $|k_{rem}|$ greater than 0.22. With somewhat higher densities a value of $|k_{rem}|$ of about 0.25 can be attained. Given optimum initial polarization (see fig. 4), $|k|$ can even be as high as 0.30.

Summarizing we can say that provided piezomagnetic ferroxcubes are specially prepared for the purpose, they can be successfully used instead of metals in ultrasonic vibrators. Another point in favour of these ferroxcube materials is that unlike the metals they involve only small amounts of expensive raw materials. In general the use of metals as piezomagnetic filter elements cannot be entertained because of their low mechanical Q (laminated vibrators) or because of their low piezomagnetic coupling (solid vibrators). Nickel-zinc ferrites can be used for the piezomagnetic filter elements provided the temperature dependence is sufficiently reduced by adding cobalt.

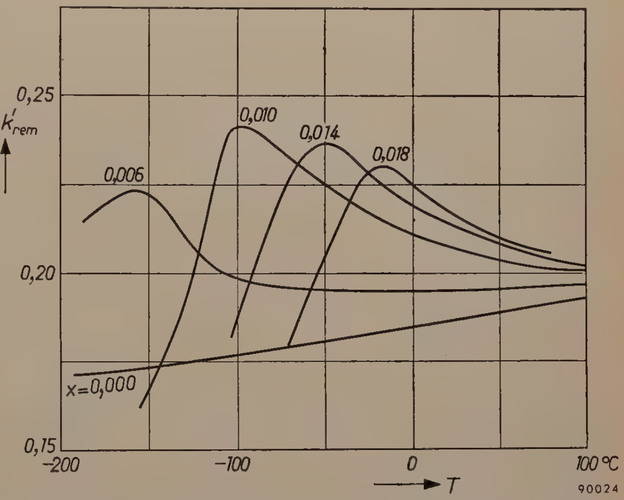

Fig. 16. Behaviour of k'_{rem} as a function of the temperature for nickel-cobalt ferrites ($Ni_{1-x}Co_xFe_2O_4$). The curves of this figure and those of figs 13 and 14 refer to rings with a porosity of 14 to 15%. For slightly smaller values of the porosity (10-12%; see also p_1 in Table II), values of k'_{rem} of approximately 0.25 may be realized at room temperature.

Summary. Piezomagnetic transducers have long been used for generating and detecting ultrasonic waves (e.g. in water). Various types of ferroxcube may be used as core material in place of piezomagnetic metals and alloys. Ferroxcube cores

need not be laminated. A short résumé is given of the piezomagnetic quantities that are relevant in this connection, and is followed by an account of the generation of piezomagnetis vibrations and a description of one or two conventional formc of transducer. The most important factors in the generation of acoustic waves are the electroacoustic efficiency and the maximum safe radiation intensity. For vibration frequencies above 20 kc/s the electroacoustic efficiency (measured at the optimum frequency) is higher for ferroxcube than for metals, since there are no eddy currents and since, in the absence of laminations, frictional losses are very low. The maximum safe intensity can be at least 10 W/cm² for continuous loading. In order to attain this high value, materials of good homogeneity and large saturation magnetostriction are required. Moreover, such materials require a high tensile strength; this may be achieved by suitable sintering techniques or suitable variations of the chemical compositions, which renders them less porous. High values for the piezomagnetic coupling coefficient, the mechanical Q and the magnetic Q enhance the efficiency and therefore also the maximum safe intensity, since they make for smaller thermal stresses at a given power. For pulsed operation, which avoids thermal stresses, maximum safe intensities of as much as 15-20 W/cm² can be expected.

In general the suitability of ferroxcube as a material for acoustic detectors is also determined by the above-mentioned coupling coefficient.

Unlike metals, ferroxcube vibrators can be used in electric filters, when the latter call for both a high mechanical Q (2000 to 8000) and a high coupling coefficient. This application allows only a slight variation in the resonance and anti-resonance frequencies with temperature. By adding cobalt this variation can be kept within the desired limits (0.03%) for the required temperature range (20-50 °C). The addition of cobalt likewise improves the coupling coefficient, which in this way can be raised to a value at remanence nearly equal to that of the best metals in use at present (0.25).

RECTANGULAR CATHODE-RAY TUBES OF HIGH ASPECT RATIO

621.385.832

For cathode-ray tube displays which are essentially long and narrow, e.g. special type radar ("A" scan) displays, there is considerable waste of equipment space when a circular-face tube is used. Further, when several displays are observed by one operator, the distances between the individual displays are inconveniently large. A special tube with a long and narrow rectangular face (bulb

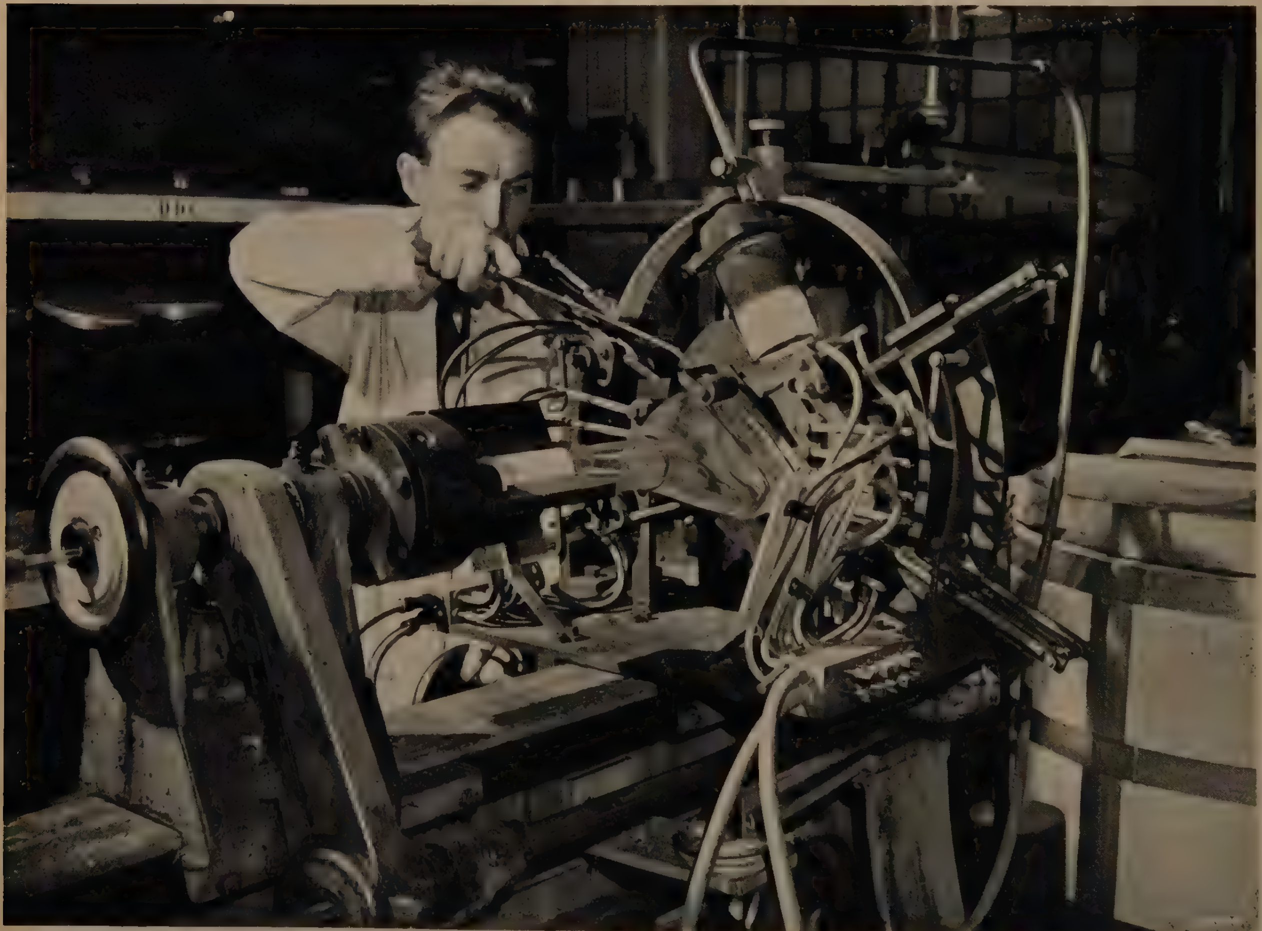

Fig. 1. Glass lathe for joining the pressed screen and cone of the rectangular cathode-ray tube bulb. The lathe contains eight stationary and four reciprocating burners. The latter are actuated by the large cam visible behind the bulb. The photograph shows the screen-cone joint during the rolling process.

periphery 156 × 66 mm, useful screen area 125 × 35 mm, i.e. an aspect ratio 3.5 : 1), has been developed for these cases. Tubes of this type permit of compact stacking and thus avoid both the disadvantages mentioned above. Some manufacturing problems not encountered in normal cathode ray tube production had to be solved for these tubes; a number of these problems will be briefly reviewed in this article.

Since it is impracticable to produce a strong enough bulb of the required shape by the usual process of blowing, the bulb design was based on the use of a pressed glass screen and cone. The depth of both screen and cone was chosen so as to permit satisfactory pressing notwithstanding their flat, narrow form; the sides of both are slightly curved for increased strength and slightly tapered for easy removal from the moulds. These requirements set a lower limit on the overall bulb dimensions for a given useful screen area.

The joints between screen and cone and between cone and neck (a length of standard 50 mm tubing) are made on a glass lathe of special design. This lathe, shown in *fig. 1*, contains four reciprocating gas-oxygen burners in addition to the usual stationary ones. The stationary burners alone would heat the corners of the glass parts less than their sides, owing to the greater peripheral speed of the former. The reciprocating burners, which are actuated by a large cam on te head stock of the lathe (see figure), increase the heating on the corners only, and produce a uniform temperature round the edges of the glass.

The phosphor coating for the screen is produced by the well-known sedimentation technique [1]). For applying the internal graphite coating, a special brush was designed whose head can be swept across the flat internal surfaces of the bulb by manipulation at its long handle.

Electrostatic deflection is usually used in tubes for this type of display. The electron gun, including the deflector plates, has to be sealed into the neck with the proper orientation, i.e. with the direction of the scan (x-trace) accurately parallel to the long axis of the rectangular screen. Setting of the gun in the correct position is effected by means of a jig, making use of the fact that the x-trace deflector plates deflect the electron beam in a direction perpendicular to the axial slot of the "interplate shield" (the latter separates the two sets of deflector plates electrostatically in order to prevent "cross-talk" between x- and y-deflection [2])). The jig is shown in *fig. 2* and the aligning procedure is explained in the caption of the figure. By this method it has been possible to maintain a tolerance of ± 2° on the angle between the x-trace and the long axis of the screen.

Before sealing the glass foot carrying the gun into the neck of the cathode ray tube, the foot must be

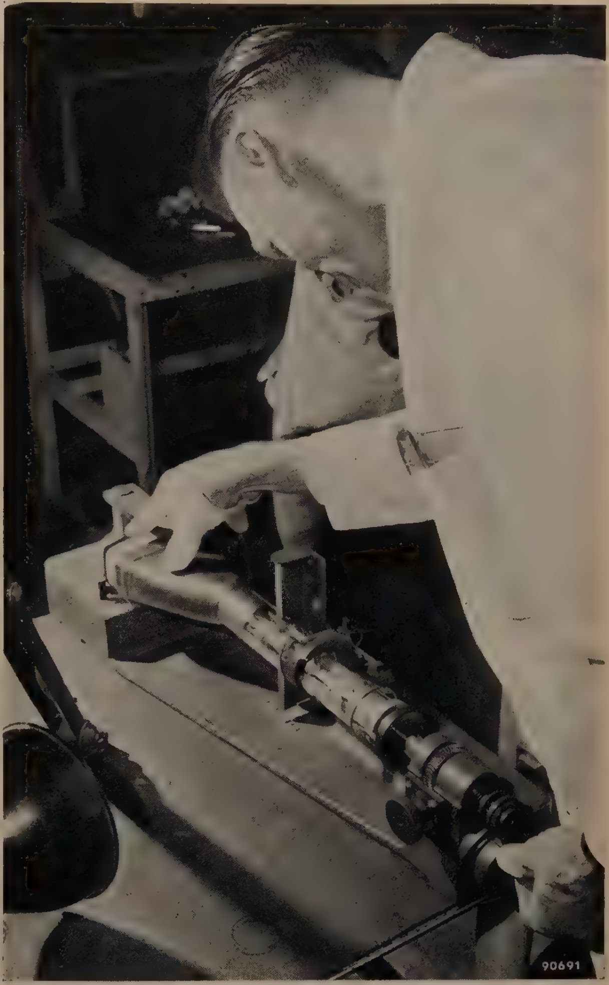

Fig. 2. Jig for adjusting the electron gun in the tube neck so that the direction of the x-trace is parallel to the long axis of the rectangular screen. The screen end of the bulb is positioned unambiguously on a heavy casting whilst the neck rests in a semi-circular support: these two locations provide a reference plane defined by the axis of the tube and the long axis of the face. At the nominal position of the interplate shield of the electron gun assembly is a bracket painted with a white reference line (broken to allow space for the tube neck). The line has the same width as the interplate shield slot and is located in a plane perpendicular to the above-mentioned reference plane. The gun assembly, which fits tightly in the neck in order to prevent its vibrating out of position in subsequent handling, is moved up the neck by the mechanism seen in the lower right part of the photograph, until the interplate shield is at the position of the reference line. The gun is then rotated until the shield slot is seen in the same straight line as the reference line. The x-deflection will then be parallel to the former reference plane and hence to the long axis of the screen.

---

[1]) See the illustrations in Philips tech. Rev. **9**, 339, 1947/48 and **10**, 306, 1948/49.

[2]) J. de Gier and A. P. van Rooy, Improvements in the construction of cathode-ray tubes, Philips tech. Rev. **9**, 180-184, 1947/48.

brought up to about 200 °C. This is usually done before insertion of the assembly into the neck, but since the aligning operation cannot be made with a hot foot, the pre-heating for the tubes described must take place with the gun and foot already in place. This is accomplished by a hot turret of steel placed around the stem. Nitrogen is passed up the stem of the foot into the bulb to prevent oxidation of the gun components. The nitrogen is pre-heated in order to avoid cracking of the hot foot.

Conventional methods are used in the further manufacturing processes such as pumping, ageing, etc.

The most important characteristics of the tube are the following: final anode voltage 5 kV, nominal screen current 10 μA with a grid drive of 17.5 V, total light intensity 0.15 candela (owing to the use of a willemite fluorescent screen of very high efficiency); nominal deflection sensitivity in the x-direction 0.19 mm/V, in the y-direction 0.21 mm/V. The line width when scanning nearly the whole screen area (describing an ellipse of 100 × 30 mm) with optimum overall focus and nominal beam intensity is 0.5 mm. This good definition, which was part of the specification for the radar applications of the tube, was obtained by a special design of the electron gun: the undeflected spot size was reduced by a high cathode loading, a high first anode voltage (1800 V) and a long focussing anode (cf. the article quoted in [2])); the deflection astigmatism was diminished as far as possible by using relatively long deflection plates with a rather large separation. Striking a suitable compromise between length and separation of the plates was facilitated by the very limited scan in the y-direction. The relatively large deflection-plate assembly called for a neat mechanical construction in order not to increase the required tube neck diameter beyond the value of 50 mm mentioned above.

F. G. BLACKLER *).

---

*) Mullard Radio Valve Co., Ltd., Mitcham (Surrey), England.

FLOODLIGHTING OF THE DUTCH NATIONAL WAR MEMORIAL IN AMSTERDAM

628.974.6.064:725.94:621.327.534.2

A National War Memorial situated in the Dam Square in Amsterdam was unveiled by Queen Juliana of the Netherlands in May 1956.

The illumination of the 22 metres high column with its statuary and the low wall that serves as background is effected by means of 30 spot-lights disposed on the roofs of neighbouring buildings. This arrangement of the sources of light is in accord with the wishes of the sculptor John Rädecker and the architect Dr. J. J. P. Oud, that the character of the monument seen by day, be as far as possible preserved when the monument is illuminated by night.

To ensure reasonable intensity of illumination at the unavoidably large distances involved (40 to 100 metres), it was necessary to concentrate as much as possible of the light from the spot-lights on to the object. On the other hand, the high luminous intensity of the light beams could not be allowed to interfere with traffic in the busy square nor could light be allowed to shine into the windows of the buildings opposite, so that the light beams had to be strictly confined to the object to be floodlit. In view of the slender form of the object it proved that the problem could be solved simply and economically by using high-pressure mercury-vapour lamps.

The lamps used are of the HPK 125 W type. The discharge is concentrated in the axis of the tube, and is about 30 × 1.5 mm in size; the mean brightness of this very elongated source is 640 stilb. The vertically disposed source is projected on the column of the monument, with a magnification of several hundred times, by means of a spherical mirror. The mirror has a sealing cover-plate which has horizontal flutes to elongate the image of the light source in a vertical direction, the source being less slender in shape than the monument. Weaker light from the outer edge of the discharge and from the quartz wall, which would pass wide of the monument, is intercepted by screens of ceramic material which are fitted close up against the discharge tube to avoid penumbrae. The HPK-type lamps were chosen with an eye to this requirement: in this type of lamp the discharge tube is exposed to the air [1]) and not mounted in an external envelope as in normal HP or HPL lamps. To ensure that the screens remain precisely in position when the tube is renewed, the construction shown in the diagram (p. 302) is employed.

The luminous flux produced by the 30 spotlights with their total power of about 4 kW is approximately 140 000 lumens; the luminance of the monument is 10 cd/m².

---

[1]) See: W. Elenbaas, Philips tech. Rev. 18, 167-172, 1956/57.

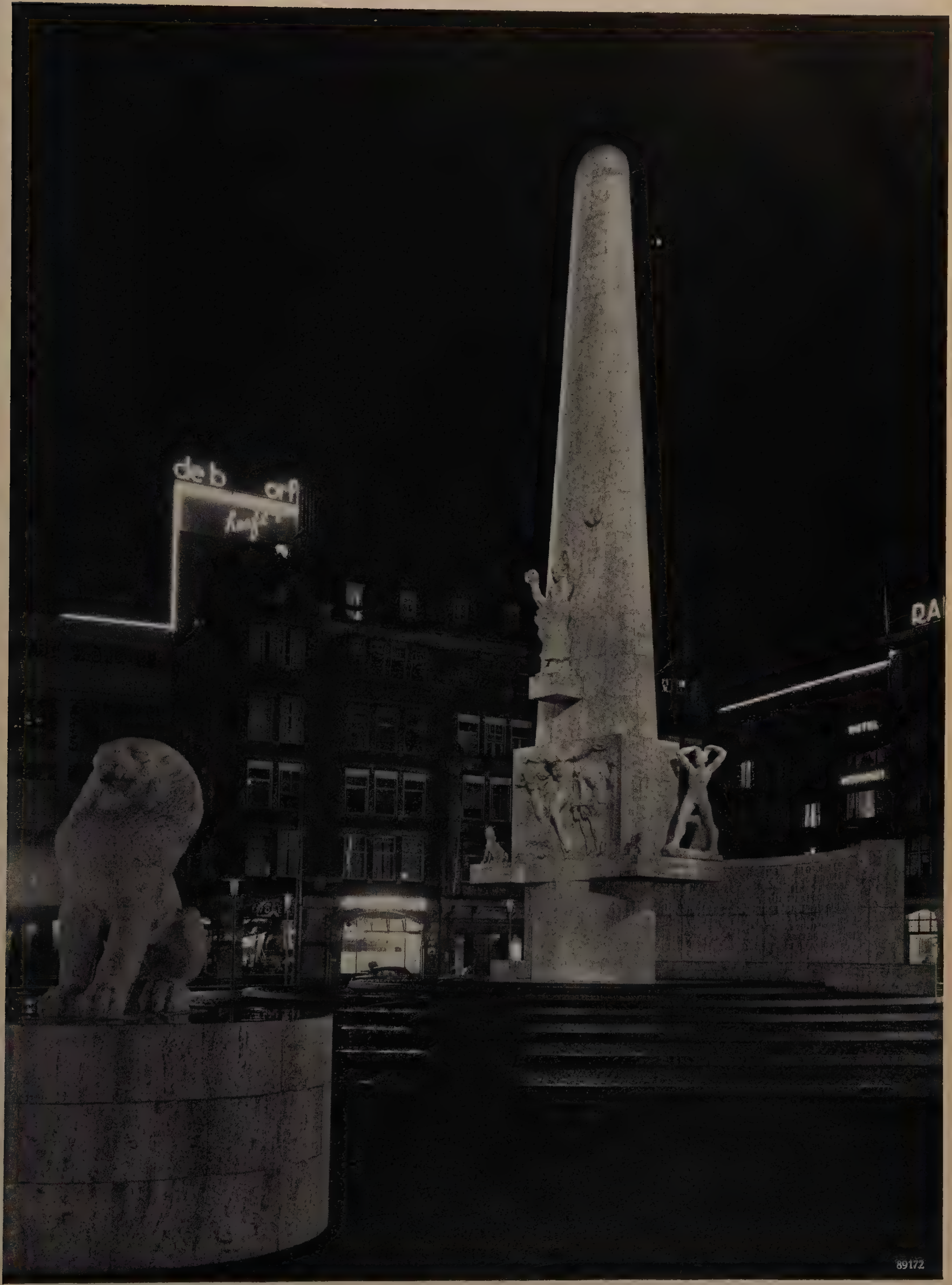
de b orf
RA
89172

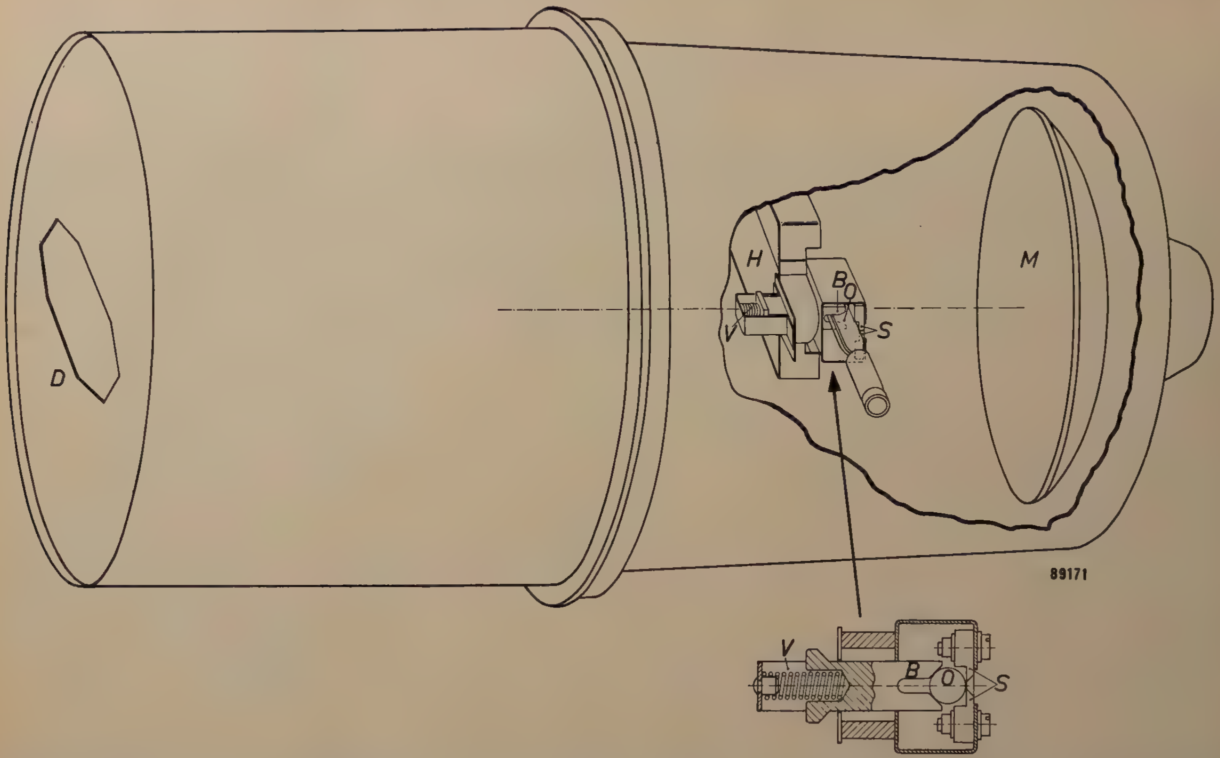

Spotlight constructed for the floodlighting of the National Monument. It is shown here turned somewhat about its axis (the discharge tube and the aperture are not vertical) and with part of the outer case cut away to reveal the HPK lamp. The discharge tube *O* of the HPK lamp rests in a ceramic block *B* which is pressed against the ceramic screens *S* by a spring *V*. This "lamp holder" is attached to a bracket *H*, which is mounted in the spotlight and can be accurately adjusted once and for all with respect to the mirror *M* of the optical system by means of screws. The cylindrical case of this spotlight with its front aperture *D* intercepts any light that might be emitted outside the desired beam.

In order to show the floodlighting to its best possible advantage, the public lighting in the square around the monument has been altered, so that there are no bright sources of light to distract the passer-by. This has been done without conferring a lifeless character on the façades of the surrounding buildings.

The 1/50 scale model of the square (shown below) in which the monument is situated ("the Dam") was employed to good purpose in preliminary experiments relating to the modification of the street lighting and the floodlighting of the monument. These experiments were undertaken in the laboratory of the Municipal Gas and Electricity Works, Amsterdam.

M. RUTGERS van der LOEFF *) and J. B. de BOER.

---

*) Chief Engineer of the Municipal Gas and Electricity Works, Amsterdam.

SEALING AMPOULES OF LYOPHYLIZED VACCINE

The photograph shows the sealing of ampoules containing lyophylized vaccine, i.e. vaccine which has been frozen in ampoules and dried in vacuo in the frozen state. Such vaccines are used both in medical and in veterinary practice.

A LOUDSPEAKER INSTALLATION FOR HIGH-FIDELITY REPRODUCTION IN THE HOME

by G. J. BLEEKSMA and J. J. SCHURINK.

621.395.623.8

For more than a quarter of a century the normal broadcast receiver has been equipped with a single loudspeaker fitted inside the cabinet. The introduction of sets with two separate speakers, each reproducing part of the frequency spectrum on the Philips "Bi-Ampli" principle, dates only from the last few years.

The installation described in this article goes a big step further, the loudspeakers being entirely separated from the amplifying part; two low-note speakers are together housed in a special cabinet and two high-note speakers separately in their own boxes. The quality of reproduction has been remarkably improved in this way, which appears to full advantage with F.M. reception and the play-back of gramophone records or tape recordings.

A complete system for sound reproduction, from performance to play-back can be considered as a chain whose first link is formed by one or more microphones and whose final link is made up of one or more loudspeakers. In between are one or more amplifiers, and further either a radio link or some "memory" with play-back facilities. (The "memory" is normally a tape recording or a gramophone record.)

The links in this chain are not equally strong. "Strong" links are those that are unlikely to be hardly improved upon by present engineering practice. As such we may consider the condenser microphone and the amplifiers. The memory is among the weaker links. However high the quality of magnetic recordings [1]) and modern gramophone records [2]) may be, certain improvements in the step function response and in the dynamic characteristic are still desirable.

Loudspeakers too should be considered as among the weaker links. A recent development in this field forms the subject of this article. The installation described is in our opinion about the very best attainable for home entertainment that can be realized with the technical means now at our disposal.

Brief description of the installation

The installation comprises four loudspeakers, viz. two for the low notes (with a range below 420 c/s) and two for the frequency range above 420 c/s (referred to here briefly as the high range). The two low-note speakers are together housed in a corner cabinet (*fig. 1*), whilst the high-note speakers are contained in separate boxes (*fig. 2*). All these loudspeakers are fed by one amplifier (type AG 9000 or AG 9006), via a low-pass and a high-pass filter respectively.

The loudspeakers for the frequency range above 420 c/s radiate nearly all their energy in a forward direction, and for this reason they are called projectors. Separate projectors can be so placed that their sound reaches the listeners only indirectly, i.e. via one or more reflections from the walls or the ceiling of the room. The importance of this method is that it diffuses the sound, so that the result approaches far more closely the actual conditions in the concert hall. Measurements in various concert halls have revealed that at most places in the hall the greater part of the sound intensity is attributable to indirect sound and only a small part to direct radiation [3]). Similar conditions can be created in the living-room by directing the projectors at different walls of the room in such a way that the listeners are outside the direct beams (*fig. 3*). The position of the low-note cabinet is less critical, since the directions from which the low notes issue are more difficult to distinguish.

The use of two projectors, placed some distance apart from each other and from the listeners, effectively avoids the "hole-in-the-wall" effect [4]). This can be explained as follows. Let us assume that we are listening to an orchestre via one loudspeaker only. Even if the whole reproduction channel reproduced uniformly the entire frequency spectrum and were completely devoid of distortion and

---

[1]) See e.g. D. A. Snel, Philips tech. Rev. **14**, 181-190, 1952/53, and W. K. Westmijze, Philips tech. Rev. **15**, 84-96, 1953/54.

[2]) See L. Alons, Philips tech. Rev. **13**, 134-144, 1951/52, and J. L. Ooms, Philips tech. Rev. **17**, 101-109, 1955/56.

[3]) Cf. Philips tech. Rev. **17**, 258, 1955/56.

[4]) Philips tech. Rev. **17**, 171, 1955/56.

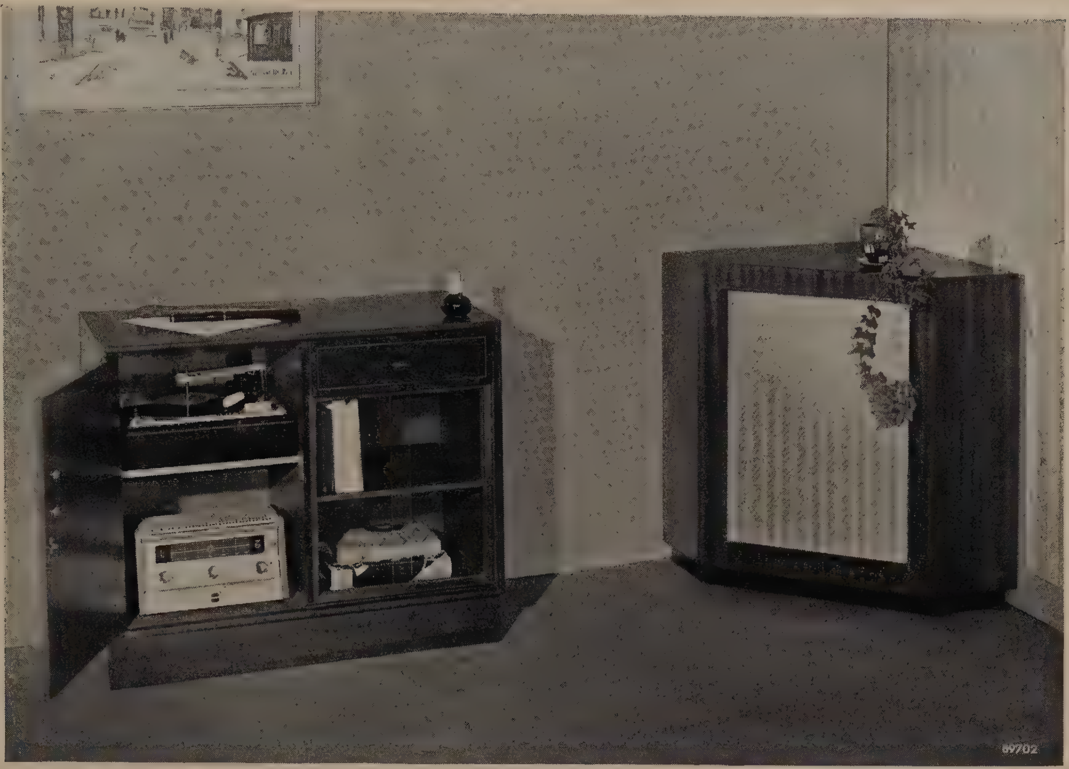

Fig. 1. Left: gramophone AG 1005 (with magnetodynamic pick-up AG 3020/21 5)) and amplifier AG 9006. Right: the low-note cabinet. The installation is completed by two separate loudspeakers for the high notes, above 420 c/s (see figs. 2 and 3).

dynamic limitations, the reproduction would still remain unsatisfactory in one respect: the entire orchestra, set up on a wide podium, would be heard as if it were compressed into the small aperture of the loudspeaker, i.e. as if the orchestra was listened to through a hole in the wall of the concert hall.

An effective means of remedying this hole-in-the-wall effect is stereophony 6), but this is only seldom used in radio broadcasts or with gramophone records. However, by placing the two projectors in such a way that the sound reaches the listeners only indirectly, the hole-in-the-wall effect can be eliminated.

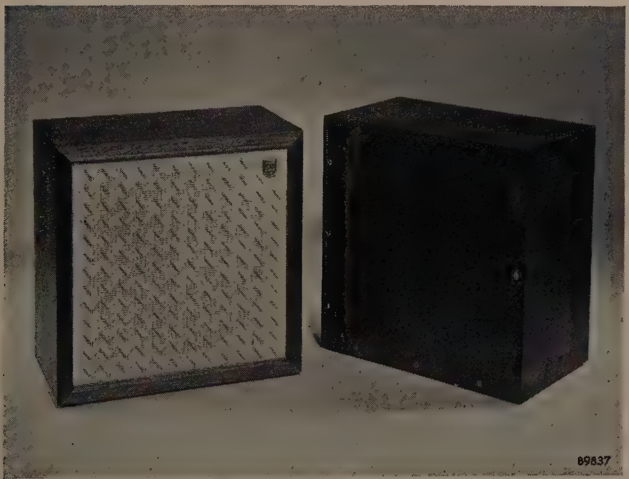

Fig. 2. The two high-note loudspeakers. Each box contains one double-cone loudspeaker and has a width and height of 26 cm.

The high-note speakers (type 9710 M) are distinguished from the low-note speakers (type 9710) in that they are double-cone loudspeakers 7). As can be seen in *fig. 4*, the moving coil drives not only a normal cone (C_1) but also a small auxiliary cone (C_2). The latter extends the frequency range, which would normally reach no further than 8 kc/s, to about 18 kc/s, and at the same time blurs the sharp outlines of the beam.

The reproduction of the high notes is further improved by the use of loudspeakers with nearly constant impedance: at 20 kc/s the impedance of a type 9710 M loudspeaker is only 1.5 times as high as at 400 c/s, whereas for conventional loudspeakers this ratio is at least 5. When fed with a constant voltage, the current flowing through such "constant-

---

5) N. Wittenberg, Philips tech. Rev. **18**, 101-109 and 173-178, 1956/57.

6) See e.g. the article quoted in 4), p. 173 et seq.

7) J. J. Schurink, Philips tech. Rev. **16**, 241-249, 1954/55.

impedance" loudspeakers will therefore decrease considerably less with rising frequency than the current flowing through conventional loudspeakers. The reproduction of the high-note range will consequently be superior, since it is the current that determines the force with which the cone is driven.

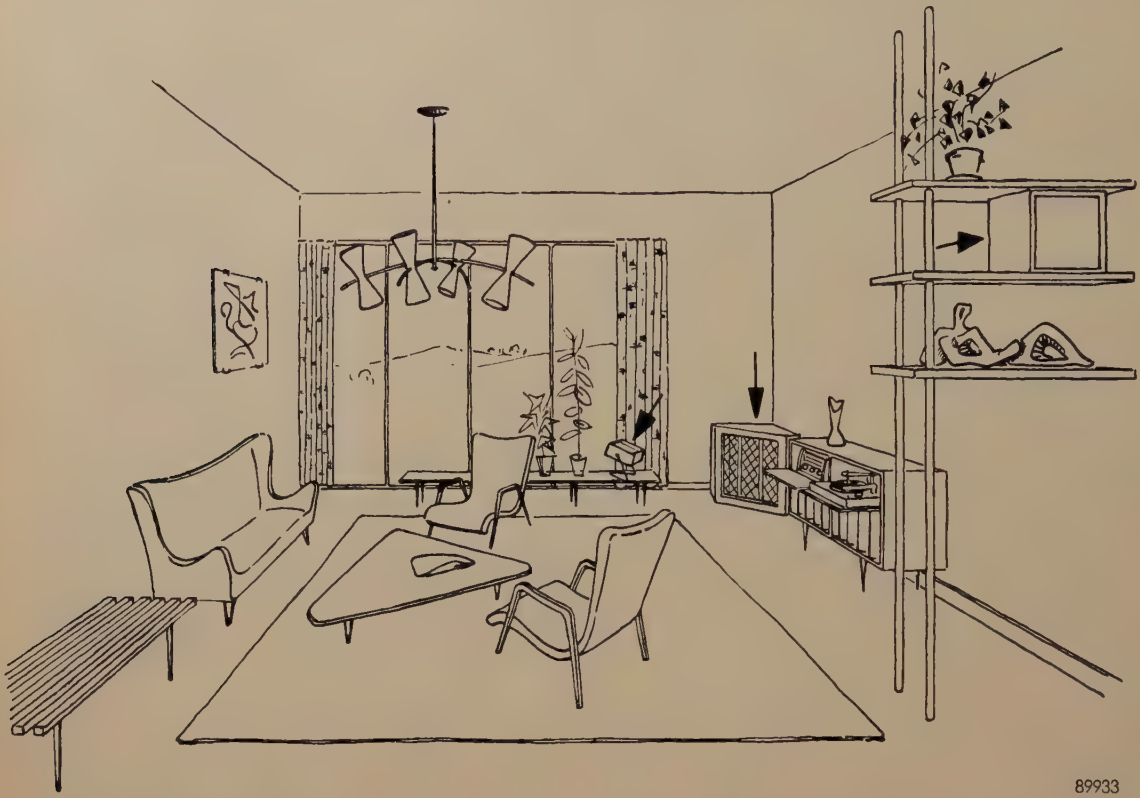

Fig. 3. A typical arrangement of the units. To the right is the cabinet containing the gramophone and the amplifier, and in the corner the low-note cabinet. The two high-note projectors are so arranged that a diffused sound is obtained.

Fig. 4. The double-cone loudspeaker 9710 M of the high-note projector. In the cross-section, C_1 is the main cone, C_2 the auxiliary inner cone, S the coil, D the centring ring, R the corrugated cone edge, M the permanent magnet, and K the copper ring ensuring a constant impedance (see further in this article). The core P of the magnetic circuit has a conical hole for accomodating the top of cone C_1.

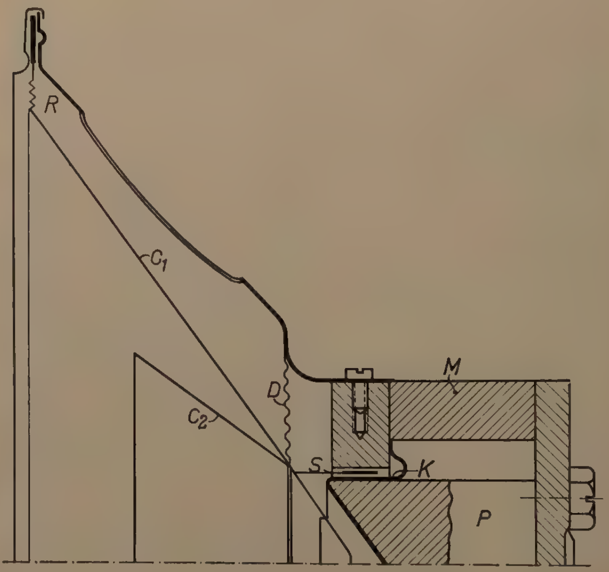

The cabinets in which the loudspeakers are housed are completely closed behind the cone. As regards the high-note projectors this prevents any back radiation (possibly directed at the listeners) which would mar the diffusion effect aimed at. As regards the low-note loudspeakers the closed box prevents the air vibrations from travelling round the cone; it thus represents an infinitely large baffle, which greatly enhances the reproduction of the very low notes. The enclosed volume of air, as we shall demonstrate later in this article, also helps in reducing non-linear distortion. To attain the best possible enclosure, "complete cones" have been used instead of the conventional truncated cone (fig. 4).

After this brief description, we shall now consider some of the above-mentioned features more closely, starting with the forms of distortion caused by non-linear phenomena.

Non-linear distortion in loudspeakers

The speech coil of a moving-coil loudspeaker, through which a current I flows, is situated in a magnetic field with an induction B. A force $F = BlI$ then operates on the coil (l denoting the length of wire in the speech coil). Since a force is numerically equal to the reaction it produces, this force is equal to the product of the mechanical impedance Z_{m} and the velocity v:

$$BlI = Z_{\mathrm{m}}\, v = \left(\mathrm{j}\omega M + \frac{1}{\mathrm{j}\omega C} + R_{\mathrm{m}}\right) v. \qquad (1)$$

In this expression ω is the angular frequency of the current, M the mass of the coil and cone and that of the air that moves with the cone, C the total compliance (i.e. the reciprocal of the stiffness) and R_{m} the mechanical resistance (both the resistance of the effective sound radiation and the mechanical loss resistance, the latter mainly occurring in the edge of the cone and in the centring ring).

The displacement x of the coil at the moment t is given by $x = \int v\, \mathrm{d}t$, and hence

$$x = \frac{v}{\mathrm{j}\omega} = \frac{BlI}{\dfrac{1}{C} - \omega^2 M + \mathrm{j}\omega R_{\mathrm{m}}}. \quad . \quad . \quad . \qquad (2)$$

The resonance frequency f_0 of the system is therefore:

$$f_0 = \frac{1}{2\pi\sqrt{MC}}. \quad . \quad . \quad . \quad . \quad . \qquad (3)$$

Because of the resistance term in (2), the displacement will be greatest at a frequency below f_0. It also appears from (2) that at frequencies that are sufficiently *above* the resonance frequency the displacement varies about proportionally with ω^{-2}, and hence by 12 dB per octave (the current remaining constant). In this frequency range the amplitude is so small that no distortion is noticeable. At frequencies sufficiently *below* the resonant frequency, however, the displacement is given by

$$x \approx CBlI. \quad . \quad . \quad . \quad . \quad . \quad . \quad . \quad . \qquad (4)$$

Here the amplitude can become so large that the relation between x and I is no longer a linear one as the result of two causes: 1) the induction B in the air-gap is not quite homogeneous, so that B depends upon x (at very large amplitudes the coil comes even partly out of the air-gap), and 2) the compliance C is dependent on x to an even higher degree. With a sinusoidal current this non-linear distortion will produce harmonics, so that the timbre of the sound will be different. Moreover, if the current consists of two (or more) sinusoidal components, non-harmonic overtones are likely to occur, which are displeasing to the ear. We shall now separately consider these two forms of distortion.

Harmonic distortion

It can be seen from *fig. 5a* that the factors B and C in (4) are not constants. The dot-dash lines of this diagram represent the force F (plotted horizontally) operating on the coil in the magnetic field, at different values of a direct current I passing through the coil. The force F is strictly proportional to I, but varies with x, since B varies with the position in the air-gap. If the field were homogeneous, all these lines would be straight and vertical. If the displacement x of the currentless coil is measured statically as a function of an external force F, we arrive at a hysteresis loop as represented by the fully drawn curve in fig. 5*a*. This shows that the total compliance C_{c} of the cone edge and the centring ring (the only compliances operative here) depends upon x and thus likewise has a non-linear character.

The variation of x as a function of time, for a sinusoidal current, can be derived from the curves in fig. 5*a*. As expected, the original sinusoidal waveform is considerably distorted and a number of higher harmonics occur in the displacement. As regards the sound pressure p, this effect will be even more pronounced since the pressure variations are proportional to $\omega^2 x$, so that the subsequent harmonics in p are respectively 1, 4, 9, ... times greater than those in x. For instance, 1% of third harmonic in x results in 9% of third harmonic in p.

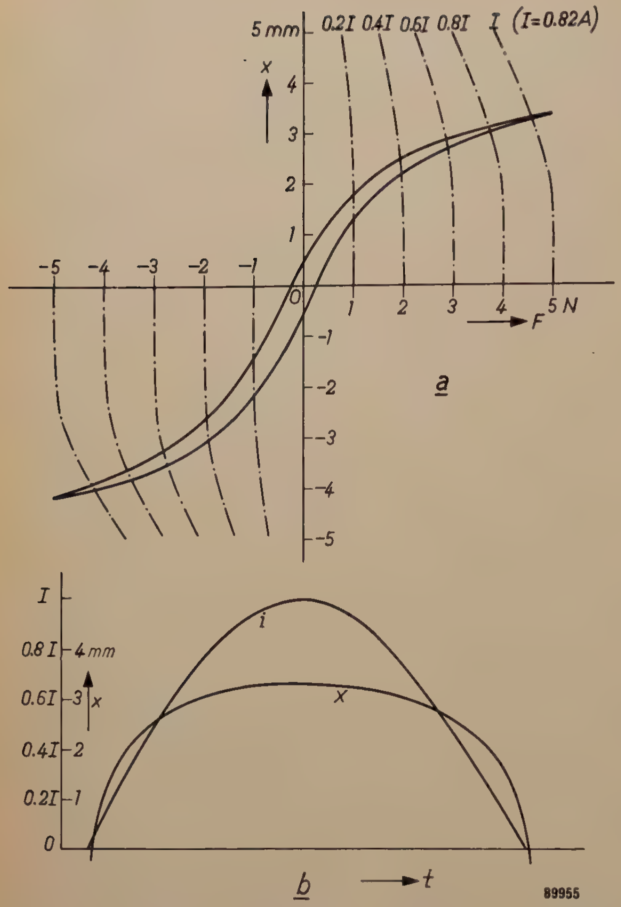

Fig. 5. *a*) Dot-dashed curves: force F on the coil of a moving-coil loudspeaker with a direct current of $^1/_5I$, $^2/_5I$, ... I passing through the coil ($I = 0.82$ A). Full curve: static displacement x of the (currentless) coil as a function of an externally applied force F.
b) Displacement x as a function of time t, showing distortion as compared with the sinusoidal current i passed through the speech coil.

Non-harmonic distortion

Let us now consider the case that the current is made up of two sinusoidal components, so that its instantaneous value i can be written as:

$$i = \hat{I}_1 \sin 2\pi f_1 t + \hat{I}_2 \sin 2\pi f_2 t \,. \quad . \quad . \quad (5)$$

The non-linear relation between displacement x and current i can be expressed by a series:

$$x = x_0 + x_1 i + x_2 i^2 + x_3 i^3 + \dots \quad . \quad . \quad (6)$$

Substituting (5) in (6) shows that the displacement will contain components with the frequencies $\pm m f_1 \pm n f_2$ (m and n being integers 0, 1, 2, ...). This effect is known as intermodulation.

The above is only valid for frequencies *below* the resonance frequency, in the so-called stiffness range, in which the amplitude is independent of the frequency. Above the stiffness range the amplitude does depend upon the frequency, which greatly complicates a quantitative evaluation. Qualitatively speaking, however, intermodulation appears here as well.

Non-harmonic distortion can be attributed to still another cause, viz. the Doppler effect. If a loudspeaker cone vibrates simultaneously with a low frequency f_1 and a higher frequency f_2, then it may be considered as a source of sound with frequency f_2 whose distance to the ear varies with the frequency f_1. Owing to the Doppler effect the pitch will then fluctuate with the rhythm of the low frequency f_1 around the higher frequency f_2, so that frequency modulation occurs. This can be interpreted as the presence of a sound with central frequency f_2 and two side-bands in which the frequencies $f_2 \pm m f_1$ occur. Let the amplitudes of the vibrations with the frequencies f_1 and f_2 be $\hat{x}_1$ and $\hat{x}_2$ respectively, then the amplitudes of the first and the second side-band components will amount to

$$10^{-2}\times\hat{x}_1 f_2\ \% \quad \text{and} \quad 5\times10^{-7}\times(\hat{x}_1 f_2)^2\ \% \quad \text{of} \quad \hat{x}_2,$$

$\hat{x}_1$ being expressed in cm and f_2 in c/s. For example, if $\hat{x}_1 = 0.1$ cm and $f_2 = 10\,000$ c/s we find: 10% for the components with the frequencies $f_2 + f_1$ and $f_2 - f_1$, and 0.5% for the components with the frequencies $f_2 + 2f_1$ and $f_2 - 2f_1$.

Means of reducing distortion

Doubling the number of loudspeakers

For reducing the non-linear distortion there exists a solution so simple that its value is not always fully appreciated. We refer to the use of more than one loudspeaker (quite apart from the separation of low and high notes). To attain an equivalent total sound volume each individual cone can then vibrate with a smaller amplitude, so that a shorter and less curved part of the hysteresis loop (fig. 5*a*) is used, and the coil operates within a more uniform magnetic field. For this reason we are using two low-note loudspeakers in our installation (the two high-note speakers are used mainly to diffuse the sound, distortion at higher frequencies being anyway very slight).

As for the low-note reproduction, this particular aim — less distortion through smaller amplitude, at equal total sound volume — might also be attained in principle by using instead of two adjacent loudspeakers with radius a (*fig. 6c*), a single loudspeaker with radius $a\sqrt{2}$ (fig. 6*b*).

Let us first compare one "small" loudspeaker (radius a, fig. 6*a*) with one "large" loudspeaker (radius $a\sqrt{2}$, fig. 6*b*). Their radiation resistances are proportional to the fourth power of their radii. The large speaker, therefore, has a radiation resistance $(\sqrt{2})^4 = 4$ times greater than that of the small loudspeaker. At the same amplitude $\hat{x}$ the large loudspeaker will radiate four times more power.

When the large loudspeaker is to be compared with a combination of two small ones then one would expect, if each small speaker, operating separately, radiates a power P, that they would produce together a power $2P$, and that therefore the large loudspeaker, with $4P$, would be twice as powerful. It should be taken into account, however, that the effect of two small loudspeakers close together is different from that of the same two speakers some distance apart. Two loudspeakers (vibrating in phase) in close proximity produce the favourable effect that they stimulate each other, as it were, to radiate a greater power.

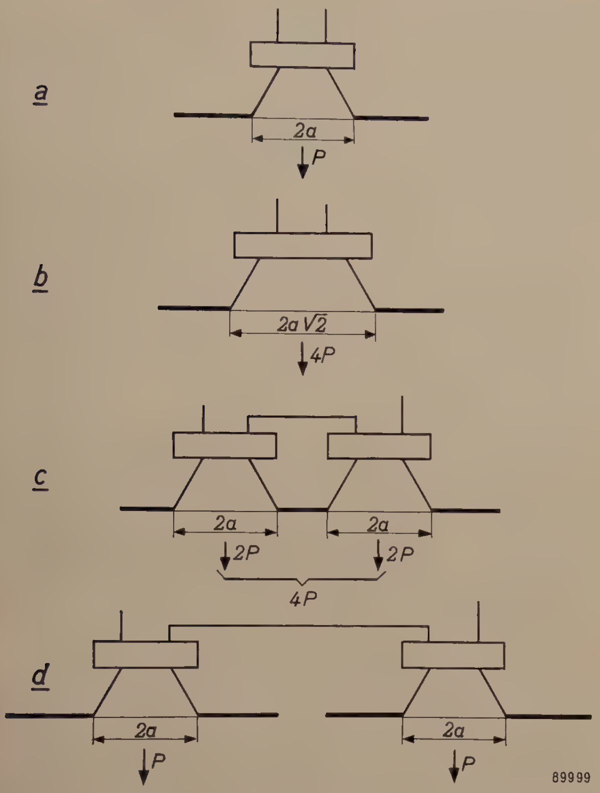

Fig. 6. *a*) Loudspeaker with diameter $2a$. The radiated sound power is P.
b) Loudspeaker with diameter $2a\sqrt{2}$. Sound power $4P$.
c) Two loudspeakers as in (*a*), placed closely together. Now either radiating a sound power $2P$, they produce together $4P$.
d) Two loudspeakers as in (*a*), placed a distance apart. As in (*a*), either produces a power P; total power $2P$.
(The loudspeakers are of course supposed to be of the same type, mounted in large baffles, and vibrating with the same amplitude $\hat{x}$.)

This effect can be readily explained as follows; if the loudspeakers are far apart (fig. 6*d*), then each yields energy to the air, since the cone is moving against self-produced pressure variations. If, however, the loudspeakers are close together (fig. 6*c*), then in addition to the self-produced pressure variations there will be those from the adjacent loudspeaker. Owing to the small distance, these pressure variations are virtually equal in amplitude and phase. Each of the cones, then, operates against a sound pressure that is twice as high and thus produces double the amount of power. The two loudspeakers together now produce a power that is twice as large as when they are placed far apart (for a constant amplitude $\hat{x}$ of the cone displacement).

Klapman has evaluated this effect for intermediate cases, viz. for two loudspeakers, considered as flat pistons (radius a, distance between centres d)[8]). *Fig. 7a* shows the curve plotted for $R_r/\varrho cA$ (R_r = radiation resistance per piston, ϱ = air density, c = velocity of sound, A = area of each piston) as a function of $2\pi fa/c$, with d as parameter. For the type 9710 loudspeaker $2a = 17.5$ cm; the frequency scales added to fig. 7 apply to this value. In the cabinet the loudspeakers are placed at a distance $d = 2.8\ a$. In the frequency range in question (below 420 c/s) R_r is substantially greater than would be the case with a single loudspeaker (curve for $d = 0$).

In the above imaginary experiment, in which two loudspeakers are brought closer together, the amplitude $\hat{x}$ was assumed to remain constant. If, however, the supply current is kept constant when the loudspeakers are approaching each other, $\hat{x}$ will decrease a little (thus reducing the advantage), because an increasing amount of air will move with the cones. This moving mass of air gives rise to a reactive component (X_r) of the mechanical impedance. The curve of this component has likewise been evaluated by Klapman (fig. 7*b*).

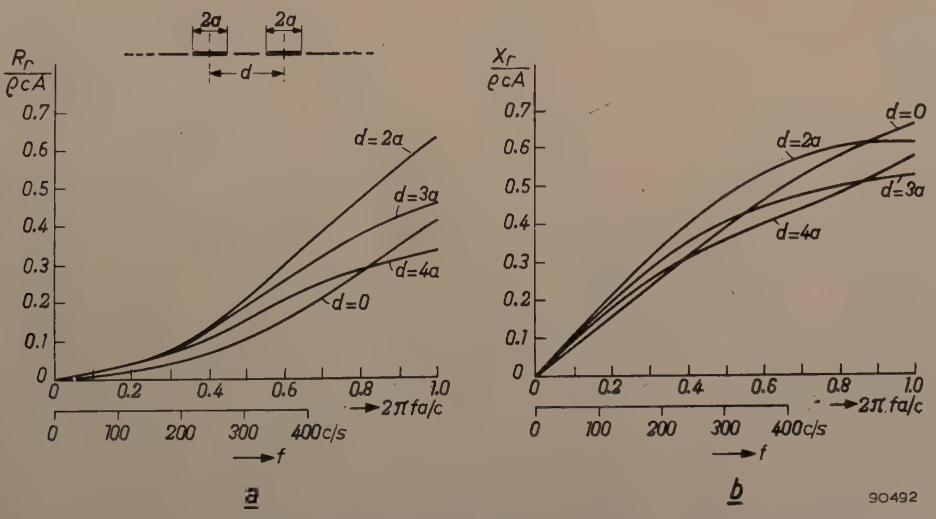

Fig. 7. *a*) The quantity $R_r/\varrho cA$, and *b*) the quantity $X_r/\varrho cA$, plotted against $2\pi fa/c$, for two circular pistons in an infinite baffle, vibrating in phase (according to Klapman [8])). The frequency scale is that for a diameter $2a = 17.5$ cm (loudspeakers 9710).

---

[8]) S. J. Klapman, Interaction impedance of a system of circular pistons, J. Acoust. Soc. Amer. **11**, 289-295, 1939/40.

A large cone, however, has the drawback that it must be relatively heavy to be sufficiently rigid. The loudspeakers used here (type 9710), with $2a = 17.5$ cm, are preferable in this respect to a loudspeaker with $2a = 17.5\sqrt{2} = 25$ cm, the cone of which is more than twice as heavy.

Loudspeakers in closed cabinets

A second means of reducing distortion is to enclose a given volume of air behind the cone. The enclosed air represents a stiffness S_a, which, unlike the rigidity S_c of cone edge and centring ring, remains satisfactorily constant and thus tends to improve the linearity of the entire system.

In order to find to what extent S_a still deviates from true linearity, we shall consider an enclosed quantity of air under a piston. If the latter is given a displacement Δx, then the air rigidity S_a exerted on the piston can be written as:

$$S_a \approx \frac{\varrho_0 c^2 A^2}{V_0}\left[1 + \tfrac{1}{2}(\varkappa + 1)\frac{A}{V_0}\Delta x\right] \quad . \; . \quad (7)$$

(the process being assumed as adiabatic). Here ϱ_0 represents the density and V_0 the volume of the air in the state of equilibrium, A the area of the piston and $\varkappa$ the ratio c_p/c_V of the specific heat of air at constant pressure to that of air at constant volume ($\varkappa \approx 1.4$).

Formula (7) can be derived as follows. An adiabatic process occurs according to

$$pV^{\varkappa} = \text{constant}$$

(p = air pressure, V = air volume). For a displacement of the piston causing the pressure to increase from p_0 to $p_0 + \Delta p$ and the volume to decrease from V_0 to $V_0 - \Delta V$, we arrive at

$$(p_0 + \Delta p)\,(V_0 - \Delta V)^{\varkappa} = p_0 V_0^{\varkappa}.$$

From this we obtain

$$\frac{\Delta p}{\Delta V} = \varkappa p_0\left[V_0^{-1} + \frac{\varkappa+1}{2!}V_0^{-2}\Delta V + \frac{(\varkappa+1)(\varkappa+2)}{3!}V_0^{-3}(\Delta V)^2 + \ldots\right].$$

The stiffness S_a can be defined as $\Delta F/\Delta x$, ΔF being the force necessary to bring about a displacement Δx of the piston. Here $\Delta F = A\Delta p$ and $\Delta x = \Delta V/A$, so that:

$$S_a = \frac{\Delta F}{\Delta x} = A^2\frac{\Delta p}{\Delta V} = \frac{\varkappa p_0 A^2}{V_0}\left[1 + \frac{\varkappa+1}{2}\frac{A}{V_0}\Delta x + \frac{(\varkappa+1)(\varkappa+2)}{6}\frac{A^2}{V_0^2}(\Delta x)^2 + (\ldots)(\Delta x)^3 + \ldots\right]. \quad (8)$$

With the help of the relation $c = \sqrt{\varkappa p_0/\varrho_0}$, the product $\varkappa p_0$ in the right-hand term of (8) can be written as $\varrho_0 c^2$. By substituting this value and disregarding the terms containing $(\Delta x)^2$, $(\Delta x)^3$, etc. in (8), we arrive at equation (7).

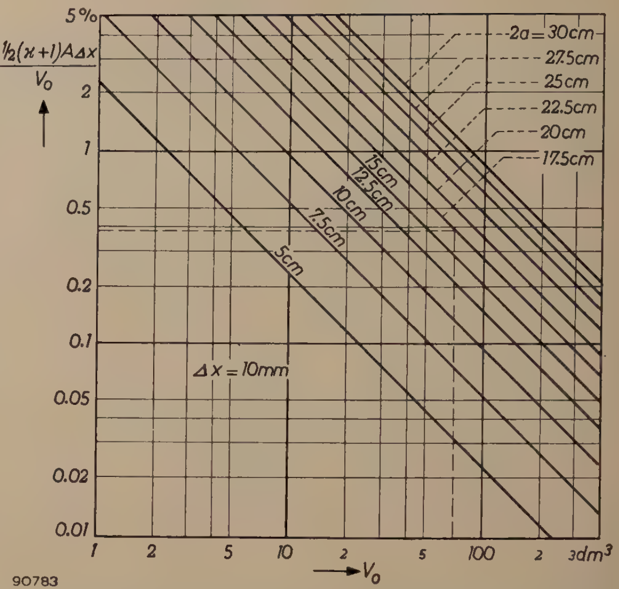

Fig. 8. The first non-linear term in the rigidity of an enclosed volume of air, $\frac{1}{2}(\varkappa + 1)A\Delta x/V_0$, as a percentage of the main term, plotted against V_0, for various values of the cone diameter $2a$, for $\Delta x = 10$ mm (see eq. 7).

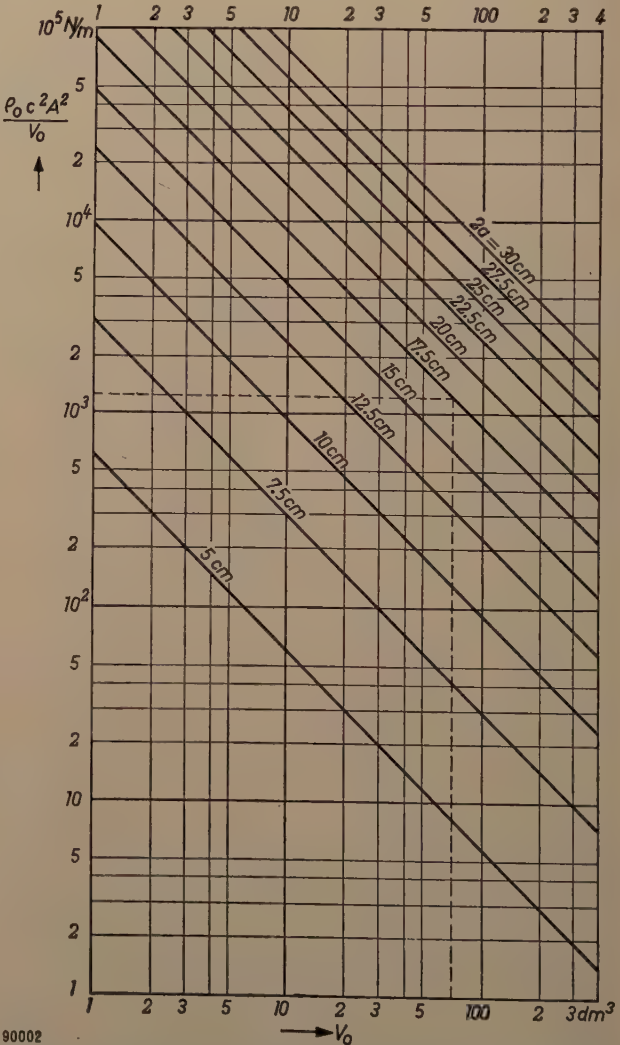

Fig. 9. Main term $\varrho_0 c^2 A^2/V_0$ of the rigidity of an enclosed volume of air (see eq. 7), versus V_0, for various values of the cone diameter $2a$.

The term $\frac{1}{2}(\varkappa + 1)A\Delta x/V_0$ represents the non-linearity of S_a. In *fig. 8* this term is expressed as a percentage and plotted as a function of the enclosed air volume V_0, with the diameter $2a$ of the cone as parameter; this diagram applies to the extremely large amplitude $\hat{x}$ (= Δx) = 10 mm. It then appears that the non-linearity in S_a can be kept below 0.5% by a proper selection of $2a$ and V_0 (e.g. $2a$ = 17.5 cm, such as that of the loudspeaker 9710, and V_0 = 70 l, which is half the volume of the low-note cabinet; this gives 70 l per loudspeaker).

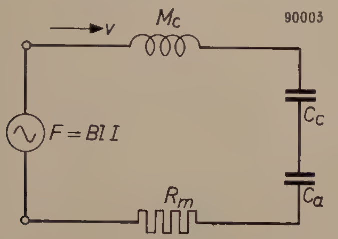

Fig. 10. Equivalent diagram of a loudspeaker with a cone compliance C_c, for a compliance C_a of the enclosed air volume behind the cone. The self-inductance M_c represents the effective mass of the cone and of the air moving with it; the resistance R_m the sum of the radiation resistance and the loss resistance.

Owing to this enclosure of a quantity of air behind the cone, the total stiffness S becomes $S_c + S_a$; the non-linearity of the cone stiffness S_c appears from the hysteresis loop in fig. 5*a*. It is evident that because S_a is virtually linear, S will show relatively less distortion than S_c, and the less so as S_a is greater and therefore as the air volume V_0 is smaller (see eq. (7) and also *fig. 9*, which represents the linear part of S_a as a function of V_0 with $2a$ as parameter).

The air rigidity cannot be indiscriminately enlarged since it is associated with an increase in the resonance frequency of the cone. This is revealed by (3), which now assumes the following form:

$$f_0 = \frac{1}{2\pi\sqrt{M\dfrac{C_c C_a}{C_c + C_a}}} = \frac{1}{2\pi\sqrt{\dfrac{M}{S_c + S_a}}}$$

($C_c = 1/S_c$ and $C_a = 1/S_a$ are the compliance values; cf. the equivalent diagram *fig. 10*). The resonance frequency lies only slightly below f_0, and the former must be confined to the lowest regions of the frequency range to be reproduced. The resonance frequency of the type 9710 loudspeakers without cabinet is about 40 c/s. The cabinet for the low-note speakers (fig. 1) is made so large (70 l per loudspeaker) that S_a considerably exceeds S_c (S_a = 1200 N/m, S_c = 750 N/m). This has raised the resonance frequency to about 60 c/s. By using electric damping (cf. the section *The amplifier* at the end of this article) this resonance peak has been sufficiently flattened out.

The high-note speakers are likewise accommodated in closed boxes, but here the object is to prevent back radiation. The boxes can be small (fig. 2) — and therefore the air rigidity great — since the resonance frequency of these speakers can quite permissibly be raised to about 300 c/s. In fact, a high resonance frequency is an advantage since it helps to suppress low notes, and so reinforces the effect of the electric filter, to be discussed presently.

Division of the frequency range

In the foregoing, intermodulation and Doppler effect were mentioned as causes of non-harmonic distortion. Both can be effectively combated by splitting up the audio range and reproducing it by separate loudspeakers.

It was found that in practice a division into *two* parts, as applied in the installation discussed here, is sufficient. As to the question at what frequency this division can best be made, it was decided to make the cross-over frequency 420 c/s. Combination tones of the type $\pm mf_1 \pm nf_2$, where f_1 is low (e.g. 50 c/s), are especially objectionable if f_2 is higher than about 400 c/s, so that the cross-over frequency should preferably not be fixed much higher than this value.

The filter effecting the separation of the high and low notes consists of two coils with self-inductance L and two capacitors of capacitance C, connected as shown in *fig. 11*. The impedance of each of the speakers is a nearly frequency-independent resistance R_1, amounting to 7 Ω for the low-impedance speakers, and to 400 or 800 Ω for the high-impedance ones. (How this constant impedance has been achieved will be discussed later in this article.) Let the internal resistance of the amplifier be negligible, and E be its output voltage; we then find for the

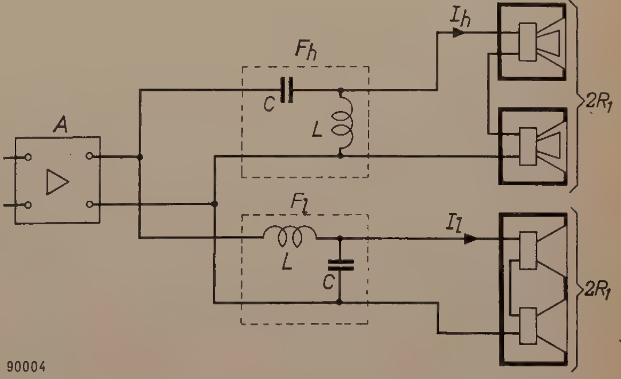

Fig. 11. F_l low-pass filter ($f <$ 420 c/s), F_h high-pass filter ($f >$ 420 c/s), A amplifier. For loudspeakers with a resistance R_1 = 7 Ω, L = 7.4 mH and C = 20 μF.

current I_l through the low-note speakers and I_h through the high-note projectors:

$$I_l = \frac{E}{2\,(1-\omega^2 LC)\,R_1 + j\omega L}$$

and

$$I_h = \frac{E}{2\left(1-\dfrac{1}{\omega^2 LC}\right)R_1 - \dfrac{j}{\omega C}}.$$

The formulae may be written as:

$$I_l = \frac{E/2R_1}{\sqrt{\left\{1-\left(\dfrac{\omega}{\omega_0}\right)^2\right\}^2 + \left(\dfrac{\omega}{\omega_0}\,\delta\right)^2}} \quad . \; . \quad (9)$$

and

$$I_h = \frac{E/2R_1}{\sqrt{\left\{1-\left(\dfrac{\omega_0}{\omega}\right)^2\right\}^2 + \left(\dfrac{\omega_0}{\omega}\,\delta\right)^2}}, \quad . \; . \quad (10)$$

where

$$\omega_0^{\,2} = \frac{1}{LC}$$

and

$$\delta = \frac{1}{2R_1}\sqrt{\frac{L}{C}}, \quad . \; . \; . \; . \; . \; . \quad (11)$$

δ being the damping factor.

In order to give each network the desired pass band (*fig. 12*), L and C must be so chosen that

$$\frac{1}{2\pi\sqrt{LC}} = 420 \text{ c/s}, \quad . \; . \; . \quad (12)$$

and there must also be adequate damping δ. For critical damping (aperiodic system without free vibrations), δ must be at least 2. In that case, however, the currents I_l and I_h are insufficiently constant in their pass bands; at the cross-over frequency they will drop by as much as 6 dB below the value $E/2R_1$ which they respectively assume at very low and very high frequencies (see the dotted curves in fig. 12). For obtaining a flatter characteristic we have preferred a somewhat smaller damping, viz. $\delta = \sqrt{2}$. The fully drawn curves in fig. 12, which drop only 3 dB below $E/2R_1$ at the cross-over frequency, represent this damping value. Outside the pass bands the drop in the curves approaches 12 dB per octave, i.e. I_l decreases at high frequencies proportionally to f^{-2} and I_h increases at low frequencies proportionally to f^2, which is also apparent from the formulae (9) and (10).

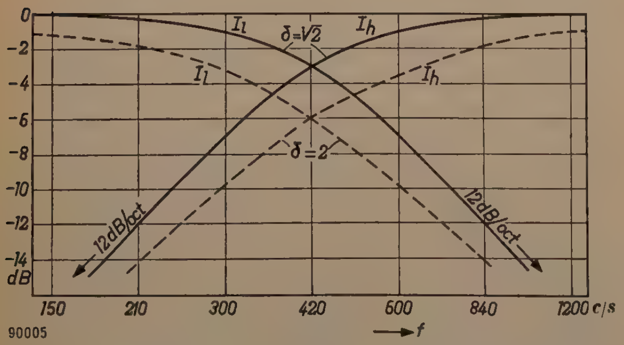

Fig. 12. Currents I_l and I_h through the low-note and high-note loudspeakers respectively, plotted against the frequency f, for a constant signal voltage and a negligible internal resistance of the amplifier, both scales being logarithmic. The dotted curves apply for critical damping ($\delta_{cr} = 2$), the full curves for $\delta = \sqrt{2}$.

If R_1 is known, L and C are completely determined by (11), (12) and the value selected for δ. For example, when $R_1 = 7\ \Omega$ we find: $L = 7.4$ mH and $C = 20\ \mu$F, which are the values used for low-impedance loudspeakers.

Some further details regarding the cabinets

One advantage of operating the loudspeakers in completely enclosed cabinets is, as we demonstrated earlier, a reduction of distortion, as a result of the additional air rigidity. Another advantage, at least as regards the low notes, is the fact that the sound waves cannot travel around the cone (the same as if the baffle were infinitely large). This latter point may be elucidated as follows.

The sound radiation of a vibrating diaphragm is impaired if the air vibrations are allowed to travel along a short path around the diaphragm. This is why this path is usually lengthened by placing the diaphragm in a baffle [9]), e.g. inside a cabinet. Let l_0 be the shortest path from the front to the rear of the diaphragm around the baffle, then we may apply the rule of thumb that the sound emission decreases by 6 dB per octave if the frequency drops below the value relating to a wavelength $\lambda = 2l_0$. For a frequency of 50 c/s, for instance, the wavelength is more than 6 m. An enormous baffle would thus be required for a satisfactory reproduction of very low notes.

In the installation described here this has been circumvented by fitting the bass-note speakers in a completely enclosed cabinet which, just as an infinite baffle, prevents even the longest waves from travelling around.

With any cabinet, however, whether closed or not, there is a risk that it will act as a resonant cavity and give rise to standing waves due to reflection against the walls of the cabinet. This has been avoided by covering the interior of both the high and the low-note cabinets with a sound-absorbent material.

---

[9]) See e.g. Th. van Urk and R. Vermeulen, Philips tech. Rev. 4, 213-222, 1939.

No special problems were involved in this procedure for the high-note cabinet, since there are several materials commercially available that adequately absorb the higher audio frequencies. For the lower frequencies, however, the solution was not so simple. In this case the principle of "panel resonance" was adopted. The inside of the cabinet was fitted with panels mounted on a framework of laths, leaving an air cushion between these panels and the walls of the cabinet (*fig. 13*). Owing to the resonator interaction of the mass of the panel with the stiffness of the air cushion, an adequate absorption through the low-note range is achieved, mainly as a result of the dissipation in the clamped-in edges of the vibrating panels. The panels, consisting of an absorbent material, furthermore bring about ordinary absorption in the upper part of the low-note range.

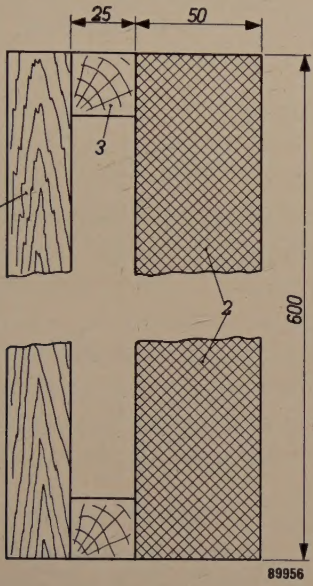

Fig. 13. Standing waves have been avoided in the low-note cabinet by fitting the inside of the walls *1* with panels *2* of absorbent material. The spacing laths *3* provide for an air cushion between wall and panel. Dimensions in mm.

There must be sufficient absorption over a certain frequency range. This range is determined by the following. The most important of the natural vibrations of the cabinet are those for which $\lambda/4$ or $\lambda/2$ is equal to one of the interior dimensions of the cabinet. The largest interior dimension is 70 cm, so that the lowest frequency of the natural vibrations is $c/(4 \times 0.70) = 120$ c/s. By giving the panels a natural frequency $f_\mathrm{p} = 240$ c/s and making this resonance not very selective, adequate absorption is obtained in the entire range from 120 to 420 c/s (in the upper part of this range, assisted by the absorption of the material itself). In connection with dimensioning the resonator such that $f_\mathrm{p} = 240$ c/s, the following should be pointed out. By analogy with eq. (3), we may write:

$$f_\mathrm{p} = \frac{1}{2\pi}\sqrt{\frac{S}{M}}. \quad \ldots \ldots \quad (13)$$

S represents mainly the stiffness S_a of the air cushion behind the panel, M mainly the mass M_p of the panel; the stiffness of the panel at the edges and the mass of the air moving with the panel may be neglected to a first approximation. According to (7), S_a can be written as

$$S_\mathrm{a} = \frac{\varrho_0 c^2 A_\mathrm{p}^2}{A_\mathrm{p} d_\mathrm{a}}, \quad \ldots \ldots \quad (14)$$

ϱ_0 being the density of the air, A_p the area of the panel and d_a the thickness of the air cushion (panel-wall distance). M_p can be written as

$$M_\mathrm{p} = A_\mathrm{p} d_\mathrm{p}\, \varrho_\mathrm{p}, \quad \ldots \ldots \quad (15)$$

d_p being the thickness of the panel and ϱ_p the density of the absorbent material. By substituting (14) and (15) in (13) we arrive at:

$$f_\mathrm{p} = \frac{c}{2\pi}\sqrt{\frac{\varrho_0}{\varrho_\mathrm{p} d_\mathrm{p} d_\mathrm{a}}}.$$

Now $c = 340$ m/s and $\varrho_0 = 1.3$ kg/m³. The density ϱ_p of the absorbent material used is 55 kg/m³. For $d_\mathrm{p} = 50$ mm and $d_\mathrm{a} = 25$ mm (fig. 13) we find $f_\mathrm{p} =$ approx. 240 c/s.

Loudspeakers with constant impedance

The self-induction of the speech coil causes its impedance to increase with the frequency (see the dotted curve in *fig. 14*). If the coil is fed with a frequency-independent voltage, the current, and consequently the force driving the cone, will decrease with increasing frequency. As mentioned in the description of the installation, the loudspeakers used have a virtually constant impedance. This is owing to the introduction of a copper ring (K, fig. 4) within the coil. This ring operates as a short-circuited winding and thus mainly eliminates the self-induction of the coil [10]). The result is the

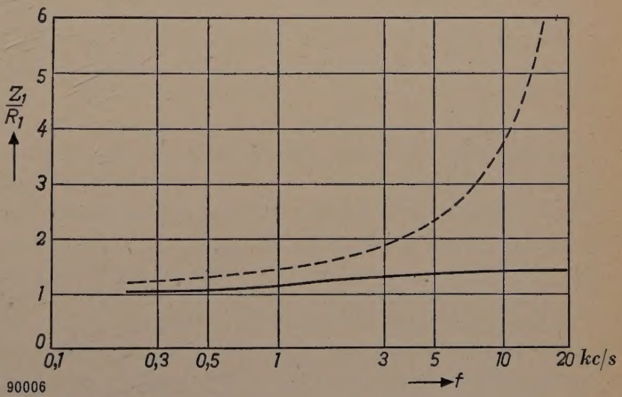

Fig. 14. Impedance Z_1 of a loudspeaker divided by the D.C. resistance R_1, as a function of the frequency f. Ordinary loudspeaker: dotted curve; loudspeaker with short-circuiting ring: full curve.

---

[10]) A ring of this type was mentioned in the Philips tech. Rev. 4, 301, 1939, footnote [1]).

impedance curve shown as the fully drawn line in fig. 14. Between the frequencies 400 c/s and 18 kc/s the impedance changes only in the ratio 1 : 1.5; without short-circuiting ring this ratio would be between 1 : 5 and 1 : 6.

The optimum shape and dimensions of the short-circuiting ring can be determined from the following analysis.

Let E_1 be the terminal voltage and I_1 the current through the coil (of resistance R_1 and self-inductance L_1), and I_2 the current induced in the short-circuiting ring (of resistance R_2 and self-inductance L_2); the impedance $Z_1 = E_1/I_1$ of the coil is then given by:

$$Z_1 = R_1 + \frac{k^2 L_1 R_2/L_2}{1+\left(\frac{R_2}{\omega L_2}\right)^2} + \mathrm{j}\omega L_1 \left[1 - \frac{k^2}{1+\left(\frac{R_2}{\omega L_2}\right)^2}\right] + Z'. \quad (16)$$

In this equation k represents the coupling factor $= \sqrt{M_k^2/L_1L_2}$ (M_k being the mutual induction between coil and ring), and Z' represents a term accounting for the e.m.f. induced in the moving coil. The motion of the coil, however, does not alter the alternating flux linked by the ring. In order to determine the influence of the ring on the impedance of the coil it is therefore permissible to consider the coil as being stationary, i.e. to put $Z' = 0$; to distinguish Z_1 in this case we shall call it Z_{10}. As regards "low" frequencies ($\omega \ll R_2/L_2$), equation (16) can be written as

$$Z_{10} \approx R_1 + \mathrm{j}\omega L_1, \quad . \quad . \quad . \quad . \quad . \quad . \quad . \quad (16a)$$

and as regards "high" frequencies ($\omega \gg R_2/L_2$) as

$$Z_{10} \approx (R_1 + k^2 L_1 R_2/L_2) + \mathrm{j}(1-k^2)\,\omega L_1. \quad . \quad (16b)$$

The dimensions of the ring should be such that the following conditions are satisfied:

1) The frequency at which $\omega L_2 = R_2$ must be so low that ωL_1 is still small with respect to R_1 (e.g. below 2 kc/s), so that at "low" frequencies (see eq. (16a)) $Z_{10} \approx R_1$.
2) The coupling between ring and coil must be very tight, so that the factor $(1 - k^2)$ in (16b) is sufficiently small to keep the term $(1 - k^2)\omega L_1$ small with respect to the resistance term up to the highest audio frequencies.

Both requirements can be satisfactorily met. It should be noted that compliance with 1) means that also the quantity $k^2 L_1 R_2/L_2$ by which the resistance term in (16b) differs from R_1, is small with respect to R_1. With an appropriately dimensioned ring, therefore, the efficiency of the loudspeaker is not appreciably reduced.

The question arises whether, with a loudspeaker without copper ring, the two soft-iron boundaries of the air-gap would not act as short-circuiting rings. This effect, however, is negligible, owing to the skin effect, which is far more pronounced in iron, with its fairly high permeability and rather poor conductivity, than in copper. With the copper ring no skin effect is noticeable since the penetration depth of the current is greater than the thickness of the ring, even at 20 kc/s. This means that the current is virtually uniformly distributed over the cross-section of the ring, so that R_2 is practically equal to the D.C. resistance of the ring.

The amplifier

As mentioned above, the bass-note loudspeakers in their cabinet show a mild resonance peak around 60 c/s. To provide a further damping of this resonance, the amplifier should have a low internal resistance.

The influence of the internal resistance upon the damping can be explained as follows. Owing to the motion of the coil (wire length l, velocity v) an e.m.f. Blv is induced in it. This e.m.f. operates on the resistance R_1 of the coil in series with the internal resistance R_i of the amplifier (R_i measured at the output terminals). These two resistances thus have to dissipate a power $(Blv)^2/(R_1 + R_i)$. Instead of this, let us imagine an equal dissipation in an imaginary *mechanical* resistance R_m':

$$\frac{(Blv)^2}{R_1 + R_i} = R_m' \, v^2,$$

and hence

$$R_m' = \frac{B^2 l^2}{R_1 + R_i}.$$

The mechanical damping resistance already present is consequently raised by this amount, R_m' being larger the lower the internal resistance R_i of the amplifier.

An effective means of reducing the internal resistance is the use of voltage feed-back, i.e. part of the output voltage is applied in anti-phase to the input voltage of the output stage or of a previous stage [11]).

The splitting-up into two frequency ranges *after* the amplifier requires an amplifier that is adequately designed to prevent any appreciable intermodulation. The amplifiers AG 9000 and AG 9006 (fig. 1) are very suitable in this respect, respectively supplying 10 and 20 W output at 2% intermodulation. The former amplifier has been designed for loudspeakers with the conventional low resistance (two 7 Ω speakers in series) and is therefore equipped with a step-down output transformer. The amplifier AG 9006, on the other hand, contains a novel output circuit, capable of directly feeding high-impedance loudspeakers [12]); the output transformer with its inevitable distortion is thus obviated here.

---

[11]) B. D. H. Tellegen, Philips tech. Rev. 2, 289-294, 1937.

[12]) An article on output circuits for high-impedance loudspeakers will appear shortly in this Review.

Summary. The high-fidelity loudspeaker installation for the home described here comprises a corner cabinet with two bass-note loudspeakers, two separate boxes for the higher frequencies, each containing a double-cone loudspeaker, and filters for splitting up the audio spectrum into two ranges, one below and one above 420 c/s. By appropriately positioning the high-note loudspeakers, good diffusion of the sound can be achieved. The listener then hears mainly indirect sound, just as in the concert hall. The so-called hole-in-the-wall effect, which is a drawback of reproduction by a single loudspeaker, is thus eliminated.

One cause of non-linearity in moving-coil loudspeakers is the amplitude-dependence of the stiffness of the cone suspension. The influence of this has been greatly reduced, 1) by doubling the number of loudspeakers, so that the cones can vibrate with a smaller amplitude, and 2) by adding a considerable, practically linear air stiffness. The latter was achieved by using completely closed cabinets. For low-note reproduction this has the additional advantage that the air waves cannot travel around the cone, whilst the high-note speakers will not emit any sound to the rear. Standing waves inside the cabinet are prevented by lining the cabinets with an absorbent material (in the low-note cabinet in the form of panels separated from the walls by an air cushion). Non-harmonic distortions (intermodulation and Doppler effect) have been greatly reduced by dividing the total frequency range into two parts. The overall reproduction extends from about 20 c/s to about 18 kc/s, the high upper limit resulting from the use of double-cone loudspeakers. Inside the coil of the loudspeakers is a fixed short-circuited ring, which virtually eliminates the self-inductance of the coil, so that the impedance rises only very little with the frequency. The amplifier feeding the installation should have a low internal resistance, which can be achieved by voltage feedback. Amplifiers type AG 9000 and AG 9006 are very suitable in this respect.

ABSTRACTS OF RECENT SCIENTIFIC PUPLICATIONS BY THE STAFF OF N.V. PHILIPS' GLOEILAMPENFABRIEKEN

Reprints of these papers not marked with an asterisk * can be obtained free of charge upon application to the Philips Research Laboratory, Eindhoven, Netherlands.

2393: H. B. G. Casimir: Anticipations . . . a continental view of physics and its future (Physics Today **9**, April 1956, pp. 13-16).

General remarks on the state of fundamental physical research in Europe and elsewhere. The author discusses some of the conditions under which research is pursued, its changing background and organization, the problem of language and the present shortage of theoretical physicists in Europe. The article concludes with some remarks on the aims and responsibilities of physicists.

2394: P. C. van der Willigen and L. F. Defize: CO_2-booglassen van staal (Lastechniek **22**, 69-77, 1956). (CO_2 arc welding of steel; in Dutch).

Arc welding in a CO_2 atmosphere can be used on various types of mild steel, including (according to the investigations reported here) rimmed steel, provided that the consumable electrode contains sufficient de-oxidizing elements. The remarkable transfer of the droplets across the arc has been studied using a high-speed camera. Because the whole CO_2 welding process is chemically relatively simple, quantitative measurements can be made from which a good picture is obtained of the various reactions. It was found that welding in CO_2 is about "equivalent" to welding in argon + 9% oxygen, with the exception of the reaction which takes place with carbon. During welding, about $2^1/_2$% CO does not react with the oxygen from the air (calculated on the CO_2 being used). The main features of CO_2 arc welding are: absence of hydrogen, low nitrogen content of the weld, less trouble with the arc length in comparison with argon, very deep penetration which shows a U-form. Because of the latter feature unbevelled butt welds can be made with low heat input and low wire consumption. CO_2 arc welding can be performed more easily by machine welding than by hand welding, mainly because of the remarkable metal transfer, the very short arc and the high travel speeds.

2395: H. Rinia: Optics in television (Problems in contemporary optics, Istituto Nazionale di Ottica, Arcetri-Firenze, 1956, pp. 492-507).

Television, which is primarily an electronic technique, has caused a renewed interest in optical problems. It has led to a demand for certain optical systems: Schmidt systems, variable-focus lenses and dichroic mirrors are examples. Television optics has introduced a new stimulus into the already existing question as to how to judge the performance of an optical system. Finally television techniques may provide new tools for optics.

2396: J. L. Meijering and H. K. Hardy: Closed miscibility gaps in ternary and quaternary regular alloy solutions (Acta metallurgica **4**, 249-256, 1956).

Although the regular-solution model is only an approximation, it may yield useful semi-quantitative results in predicting the form of ternary miscibility gaps from binary data. The spinodal equation of quaternary regular solutions has been derived and the coordinates of second-order critical points are given as a function of the six binary interaction parameters. Quaternary critical points are of special interest, as they are connected with closed miscibility gaps. The conditions which cause a ternary critical temperature to be raised by the addition of a fourth component are given. The results are applied to miscibility gaps in liquid and f.c.c. alloys.

2397: J. L. Meijering: On thermodynamical analysis by calorimetry alone (Acta metallurgica 4, 333-335, 1956).

Letter in which the author discusses and supports the plea of Oelsen, Schürmann and Heynert for thermodynamical analysis by purely calorimetric methods. Some extensions of this idea are put forward.

R 300: P. Zalm: The electroluminescence of ZnS type phosphors (Philips Res. Rep. 11, 417-451, 1956).

Continuation of **R 298**. In section 4 of this paper it is shown that the voltage dependence of the emittance is due to the presence of a Mott-Schottky barrier and may be expressed by $H = H_0 \exp(-cV^{-\frac{1}{2}})$. A theoretical model is drawn up for crystals embedded in a dielectric. This is tested against a number of experimental results reported in section 5 of the paper. Finally a study is made of the energy efficiency of electroluminescent phosphors.

R 301: J. Volger and J. M. Stevels: Further experimental investigation of the dielectric losses of various glasses at low temperatures (Philips Res. Rep. 11, 452-470, 1956).

The results of loss measurements at low temperatures on a number of glasses are given. These are discussed qualitatively in connection with the glass structure. The importance of impurities in fused silica is shown. The influence of thermal treatment is also considered. Contrary to experience with quartz crystals, no effect of irradiation (formation of colour centres) upon the dielectric losses at low temperatures is found. A comparative survey of the various loss mechanisms found hitherto in the vitreous and crystalline states is given.

R 302: W. Ch. van Geel and C. A. Pistorius: On the residual voltage with electrolytic capacitors (Philips Res. Rep. 11, 471-478, 1956).

After an electrolytic capacitor, e.g., Al/Al_2O_3/electrolyte, has been charged and discharged, a voltage is found to develop anew across the capacitor plates. This is called the residual voltage, and it is found to be proportional to the product of the field strength in the oxide layer and the thickness of this layer. It is assumed that Al^{3+} ions in the lattice have moved to adjacent positions, considering the fact that there is a large number of vacancies in the Al_2O_3 lattice. A simple computation shows that for an average shift of an Al^{3+} ion over a distance of 2 Å, 0.1% of the available Al^{3+}ions have been displaced.

R 303: C. Z. van Doorn and Y. Haven: Absorption and luminescence of colour centres in KCl and NaCl (Philips Res. Rep. 11, 479-488, 1956).

Crystals of KCl and NaCl, coloured additively and quenched from high temperature to liquid-nitrogen temperature, show the *F*-absorption band and when irradiated in this band an emission in the infrared. If kept for a short time at room temperature a new absorption band (*M*-band) develops and irradiation in this band gives rise to a new emission band. If an *M*-absorption band is present, this new emission band is also found when the crystal is irradiated in the *F*-band. An explanation for this is offered. After long periods of ageing, *R*-bands also develop; irradiation in the *R*-bands as well as in the *F*-band gives rise to a third emission band.

R 304: A. I. Luteijn and K. J. de Vos: Permanent magnets with $(BH)_{\max}$ values over ten million gauss oersteds (Philips Res. Rep. 11, 489-490, 1956).

Brief note announcing the attainment of $(BH)_{\max}$ values up to 11 million gauss oersteds at a remanence of 11800 gauss and a coercivity of 1315 oersteds in permanent magnets of "Ticonal" X (titanium-containing), by preparation in an atmosphere of pure argon, using very pure raw materials. Rods of these alloys produced by pulling from the melt contain large crystals with a [100] axis nearly parallel to the direction of pulling, and a subsequent heat treatment in a magnetic field produces the high values reported above.

R 305: J. D. Fast: The influence of impurities on the recrystallization texture of cold-rolled 3% silicon iron (Philips Res. Rep. 11, 490-491, 1956).

In the preparation of grain-oriented silicon-iron sheet, whereby a preferred direction of magnetization is obtained by combined rolling and heat-treatment, the results are often poorly reproducible. The present note refers to an investigation which shows that the grain-orientation effect is brought about by impurities: the effect cannot be obtained in very pure silicon iron. It has been found that, in particular, small amounts of nitrogen introduced into the alloy before the cold-rolling produce a very good and reproducible texture. To achieve the optimum magnetic properties, the nitrogen must be expelled during a final heat-treatment.